Evaluating the Impact of Land Deregulation on Mediterranean Olive Groves in Jaén, Spain: From Olives to Informal Urbanization

Gianlorenzo Gual Suárez

(N°2876913)

Supervisor: Dr. Eric Koomen

Department of Spatial Economics

School of Business and Economics

Vrije Universiteit Amsterdam

August 2026

Abstract

In response to the climate induced profitability crisis of Jaén’s olive groves, the LISTA law was introduced in 2021 in the Andalusian territory, simplifying the classification of rustic land and relaxing its building regulations. This thesis evaluates the impact of this reform on land abandonment, urban sprawl probability and three-dimensional vertical growth of illegal buildings in the province of Jaén. For this purpose, data has been collected from 31,579 plots of traditional olive grove farms in 2018 across 5 different time periods (2020, 2022, 2023, 2024 and 2025). By use of GIS-software and Airborne LiDAR data (PNOA), the correspondent Normalized Digital Surface Model (nDSM or CHM) was estimated at the parcel level in order to track vertical growth of detected illegal constructions. Compared to previous studies, this analysis implements a quasi-experimental methodology at a high level of granularity across multiple dimensions of analysis. The estimated Fixed Effects (TWFE) and Linear Probability (LPM) models reveal that the LISTA law increased shrubbing in the treated observations by approximately 1.2 percentage points. However, it also reduced their urban sprawl probability by roughly 1.22 percentage points, which could be explained by the substitution effect of the ensued upzoning. The reform did not influence the vertical growth of sprawling, as illegal urban developers prefer geomorphological attributes that allow for camouflage of their building’s geometry. Understanding the distinct impact dimensions of policies, such as the LISTA law, allows for the policymakers’ deeper understanding on the role of institutions and optimal resiliency planning against the threats posed by climate change.

Keywords: land use policy, upzoning, agricultural abandonment, urban sprawl, Airborne LiDAR.

Acknowledgements

This thesis would not have been possible without their unconditional support and inspiration. First and foremost, I am grateful to my mom (Ma), dad (Pa) and sister (Fer). Y'all have showed me the true meaning of happiness and what I want to be when I grow up.

I am extremely grateful to Luisja, Nieves, Bo, Isaac, Climacot, Fer Oropizza, Mateo, Luis y Diego, Mich, Iann and Daniel; if not for the countless beers and ciggies, for the many, many laughs. Also Pau, Bas and Otis.

I would like to thank Cookie, Grisi, Spice, Nessie, Kaylie, Miel, Gato, Cuca, Merlina, Kimba and my Sam, as well as all other four-legged citizens that allowed for scritches.

I would like to show my extreme appreciation and gratefulness to my supervisor, dr. Eric Koomen, as his blunt input was critical in understanding that I understood nothing at all. I am also grateful towards dr. Saúl Basurto Hernández, dr. Luis Fernando García Covarrubias and dr. Hans Koster. If you had not believed and given me the opportunity, I would not have either.

Lastly, I would like to give my deepest appreciations to the Vrije Universiteit Fellowship Programme (VUFP) and NL Scholarships, their teams and ex-alumni, without the funds I would not have been able to eat. And Nina. Especially Wilburt.

Table of Contents

1. Introduction

Andalucía's rural rustic land has three mechanisms acting towards shaping its landscape: the constant agricultural land abandonment that has plagued it and become known as the "España Vaciada" phenomenon (Duarte et al., 2008; Perujo-Villanueva et al., 2017), the low and medium density recreational settlements that have seeped in from sprawl of secondary residences on the coast (Salvati and Gargiulo Morelli, 2014), and the institutional rigidity and inefficiency of prohibitive upzoning (Ramon y Cajal Abogados, 2021; Coppola, 2022). The Mediterranean type of sprawl is characterized by fragmented land ownership with extensive ribbon and leapfrog development (Salvati and Gargiulo Morelli, 2014).

There have been numerous policy attempts for promoting the socio-economic development of the region through the deregulation of the restrictions surrounding rustic land, the implemented reforms of December 2021 (*Ley 7/2021 de Impulso para la Sostenibilidad del Territorio de Andalucía*) are a prime example of this institutional undertaking (BOE, 2021). The LISTA law essentially simplified the classification codes for rustic land and opened a legal avenue for the construction of single-family homes unrelated to agricultural production on common rustic land parcels with specific physical parameters (BOE, 2021; SoloArquitectura, 2024).

For these reasons, this study aims to answer the following question: **to what extent did the relaxation of regulations of rustic land through the LISTA law causally affect the agricultural land abandonment and illegal urban sprawl in Jaén, Spain?**

This study uses a panel dataset that contains spatial and virtual point cloud data and applies two-way fixed effects models and linear probability models to isolate the regulatory shock of the LISTA law on Jaén's rustic land.

The aims of this study are:

1: To estimate the change in probability of agricultural land abandonment and vegetation cover change into common Mediterranean shrub. This model isolates the exogenous regulatory shock and identifies the increasing thermal stress on the workforce as a driver of low productivity and abandonment.

2. To quantify the causal effect of the LISTA law on the discontinuous residential sprawl of Jaén's rustic land. This model empirically assesses the substitution effect caused by upzoning as described in **Greenaway-McGrevy and Phillips (**2023).

3. To develop a Canopy Height Model (CHM) from three-dimensional LiDAR data in order to track the maximum height of identified illegal constructions post-reform.

The structure of this study is as follows. Chapter 2 reviews the literature on land use change, upzoning deregulation, urban sprawl and the Mediterranean type of sprawling and thermal stress as a driver for agricultural abandonment. Chapter 3 explains the methodology and develops three different models constructed to analyse the LISTA law's impact through three dimensions. In Chapter 3, the data sources to calibrate the model are presented and discussed. Chapter 4 displays the results and robustness checks of said models. Lastly, Chapter 5 concludes the study and discusses the limitations of the approach, as well as possible future research avenues.

2. Literature Review

There has been extensive analysis done on land use and land cover, as it is a highly debated subject matter in Environmental Economics and Land Change Science. Land allocation has been typically explained through bid-rent equilibriums and location models derived from Von Thünen, in which simple transport dynamics, a continuous market and a homogenous environment are assumed to reduce the complexity of an already nuanced dilemma (Walker, 2004). However, these assumptions will hamper the evaluation of certain ecosystems, such as the semiarid province of Jaén, Spain. Land allocation in these Mediterranean regions is faced by a multifaceted set of problems, including dynamic ecological processes (namely land degradation and soil erosion), institutional and regulatory rigidity, among other influencing factors (Ruz Carmona, 2025).

The second chapter of this thesis pertains to the revision of the existing empirical and theoretical literature relevant to this investigation. The implementation of the Law 7/2021 on Promoting Sustainability in the Region of Andalusia (LISTA Law) on the Jaén province came as a deregulatory shock on the province of Jaén. These changes acted on the limitations around rural non-developed land classified as rustic land, which also changed the expectations of the surrounding market.

The LISTA law and its regulations (Decree 550/2022) marked a paradigm shift in this restrictive tendency, as it drastically simplifies land classification into Urban and Rustic land; the latter is, in turn, subdivided into Protected and Common. The subclassification depends on how the property was classified and the State's determination of soil preservation for environmental or legislative purposes (Ramon y Cajal Abogados, 2021).

This law relaxes regulations around the construction of single household residencies on common rustic land. They must meet strict physical planning parameters, i.e. minimum parcel size of 2.5 hectares, building size restricted to 1% of total lot area, among others (**BOE,** 2021; **Soloarquitectura,** 2022).

In order to capture the different dimensions of the LISTA reform's effects, as well as its interaction with biophysical constraints relevant to the Jaén province, this study will focus on three distinct dimensions: the Extensive analysis, which constitutes for the dynamics of land abandonment followed by its shrubbing, the Administrative Intensive analysis examines the likelihood of a parcel being turned into illegal residential sprawl, and lastly, the Physical Intensive dimension centres around the physical scale of the detected informal buildings of these plots.

2.1 Quasi-experimental modelling and theories of Macrostructural Assignment

Land Change Science studies have two principal theoretical methodologies: Quasi-experimental modelling and theories of Macrostructural Assignment for uncovering spatial causal relationships on a microterritorial scale.

The framework laid out in Barbier et al. (2010) is fundamental for understanding land through relative rent values and institutional failures. Rudel et al. (2005) developed the theory of Forest Transition to systemize the adoption of two plausible macroeconomic explanations for the outcome on the rural population of these resource-scare marginal zones; The seize of agricultural activity as the labour force is attracted to urban and industrialized centres or subsisting through the deforestation of the region (Rudel et al., 2005). One limitation on these studies a failure to consider the mechanisms behind parcel-level spatial substitution, as long run homogenous tendencies are assumed for normative conflicts.

The implementation of quasi-experimental designs on impact evaluation was pushed by the econometric literature in order to overcome the aggregative bias.

The research done by Greenaway-Mcgrevy and Phillips (2023) and Greenaway-Mcgrevy (2023) modelled the upzoning of the recent reforms in Auckland and Lower Hutt, New Zealand through a Difference-in-Difference (DiD) design. Their studies demonstrated that the legal offer of the housing market changes with the relaxation of urban development. Michael Wiebe’s (2022) two sector model describes subsequently how, for the current non-random distribution of common rustic land, the market’s supply and profitability will decrease by illegal urban sprawl in geographically unsuitable rustic land.

2.2 The Extensive Dimension

This ambit concerns the metric used by the olive farmers to gauge the tipping point of agricultural production and transition their land into the first stages of forest cover. Numerous studies (Sánchez Martínez and Gallego Simón, 2011; Sanz-Cañada, 2014 and Ruz Carmona, 2025) have found a strong relation between the dynamics of agricultural abandonment and the structural rentability crisis of the traditional mountain olive groves, which is the main form of cultivation in the region. These mountain groves are predominantly located on steep mountain areas and low fertility soil, which conditions them, potentially stunts the orchards’ growth and entails a competitive disadvantage, as the use of heavy machinery or other large capital investments are practically impossible on slopes with a gradient of more than 20 percent because of the lack of accessibility (Ruz Carmona, 2025).

The economic sustainability of these traditional forms of agriculture depends solely upon the absorbed operational costs of each farm (Perujo-Villanueva et al., 2017). Another grave problem Jaén's olive groves face is the micro-fragmentation and spatial dispersion within a single farm. The literature consensus surrounding high fragmentation rates of agricultural lands indicates that a severe reduction of the producers' earnings takes place, which is caused by the longer transportation times and exponential increase on fuel costs and heavy machinery. This represents 25% of the total production costs of Jaén's olive farms, that result from the diminished accessibility to final markets (Perujo-Villanueva et al., 2017; Duarte et. al, 2008).

According to Duarte et. al (2008), these parcels are frequently located on marginal zones, and their economic unviability turns farmers towards other sources of income through off-farm activities and pensions. Subsidies and support for these farms eroded internationally since the olive oil regime was integrated under the single payment scheme (SPS) and excluded from the Common Agricultural Policy (PAC). As evident in the general downward trend on the market price, olive producers have been pressured and cornered towards land abandonment (Carmona-Torres et. al, 2023).

The traditional agricultural system that most farms in Jaén operate under are labour intensive and require regular maintenance and pruning of the orchards, as well as the seasonal harvesting of the crop under extreme weather conditions. Climate change has increased the frequency, duration and intensity of heat waves, particularly in southern Spain. Contemporary Land-use Change Science indicates that these extreme conditions reduce the workers' productivity (Črepinšek, Žnidaršič and Pogačar, 2023).

Traditional land abandonment models do not take into account climate change's effect on the workforce, usually only focused on the relationship with crop yield and treating the phenomenon exclusively as an agronomic variable (Duarte et al., 2008; García-Ruiz and Lana-Renault, 2011; Quintas-Soriano, Buerkert and Plieninger, 2022; Gual, 2025). The physiology of the human body seeks to maintain a stable internal temperature of around 37°C, interacting with the environment's thermal conditions. This is formalized under the body heat balance equation and is as follows (FAO, 2020):

$$S = M - W \pm E \pm R \pm C \tag{1}$$

where M represents the marginal rate of heat produced by physical exertion, W is physical labour, E is the evapotranspiration of the body (sweating), R and C are heat exchange radiation and circulation and S is the net storage of body heat (FAO, 2020). Reaching critical temperatures will reduce the effectiveness of the natural body's mechanisms for dissipating heat (specially evapotranspiration), increasing the value of S and severely reducing the worker's performance, which will also exponentially increase the risk of work accidents and heat strokes (ILO, 2019).

The academic consensus provides empirical evidence for the use of the Universal Thermal Climate Index (UTCI) for representing the worker's bioclimatic exposition to physical labour on a municipal scale. (Črepinšek, Žnidaršič & Pogačar, 2023; Occupational Heat Stress Study, 2016). The equation for the UTCI is specified as (Occupational Heat Stress Study, 2016):

$$UTCI = f(T_a, T_{mrt}, V_a, RH) \tag{2}$$

where T_a refers to the air temperature, T_{mrt} is the mean radiant temperature, V_a is the wind speed and, lastly, RH is the relative humidity of the environment (Occupational Heat Stress Study, 2016). The literature has provided concrete proof demonstrating that modelling the UTCI represents the nonlinear relations that thermal stress generates on the worker and, ultimately, reduces the supply of labour through a general decrease in the number of hours worked in high exposure zones, particularly for tropical regions (Dasgupta, 2021).

The increasing frequency of extreme weather conditions has pushed the younger population to work in non-agricultural related jobs in enclosed places with air conditioner; the vulnerable, older population of the traditional olive growers is delegated the most physically taxing tasks (Worklimate 2.0, 2024). From the farmer's perspective, it will increase the operational costs as this will result in difficult access to seasonal workers, as well as the requirement for longer break times for the workforce and a reduction in number of hours worked, thus, increasing their wages and reducing the effective labour supply (Dasgupta, 2021).

Recent studies have estimated the loss in productivity for physically heavy tasks to be around 6.5% for every °C increase in temperatures between 19.6-31.8 °C. This is shown in a potential reduction of up to 80% in labour capacity due to heat stress and exposure (Dasgupta, 2021; van Daalan et al., 2022; Worklimate 2.0, 2024).

The shrinkage in agricultural activity has accelerated the physical abandonment of plots in marginal zones which have increasingly deteriorated due to the effects of climate change. The culmination of this is the progressive advancement of shrubbing or rewilding, in other words, a passive ecological surrender (Navarro et al., 2023).

This rapid recolonization by nature is firstly done by shrub species and the Mediterranean scrubland (Ribeiro et al., 2024). In the literature surrounding the Mediterranean landscape, the consensus around this recent and continuous accumulation of dense scrubland is that it poses a hazard through vegetation flammability, increasing exponentially the risk of fire and the intensity and severity of forest fires (Baudena et al, 2020). The increase in aridity also traps the ecosystem into a permanent state of dense mediterranean shrub as it impedes the transition into forest cover (Baudena et al, 2020; Ribeiro et al., 2024).

The firefighting trap, as coined by Moreira et al. (2020), provides a feedback loop to this renaturing process. In a historical review, wildfire management policies are treated as a function of area burned by fires and have mainly focused on immediate fire suppression, while ignoring mitigation practices, including the removal of biofuel. This generates an extremely homogenous landscape, with a serious proclivity to combustion (Regos et al., 2024). It is estimated that 41% of fires occur in scrubland while only 6% occur in zones under active agroforest management (Burgess, 2021).

The consolidation of the Mediterranean shrub on these parcels is mutually and spatially exclusive with their socioeconomic advancement into productive farms, recreational or urban spaces due to the associated vegetation's high fire risk and increased cost of clearing the parcel. (Ribeiro et al., 2024; Burgess, 2021). Fire weather, defined as drought and extreme heat waves, provides the perfect conditions for uncontrollable megafires that exceed the capacity of operating fire services (Moreira et al., 2020).

2.3 The Administrative Intensive Dimension

The “Mediterranean style of sprawl” has been clearly separated in the literature from the sprawl mechanisms analysed in Anglo-Saxon countries. Described by Coppola (2022) in Italy and by Polyzos and Minetos (2007) in Greece, as low quality, discontinuous and unplanned urban growth. It has resulted in atomized, self-constructed residencies on rural areas, previously considered as non-developed agricultural plots (Polyzos and Minetos, 2007). Weak institutions and “grey governance” (selective compliance), as well as the involvement of private agents in the subdivision of informal land, have promoted and provided structural amnesty to sprawl sporadically throughout time (Coppola, 2022; Roy, 2005).

Roy’s (2005) framework establishes that the institutions control to what extent the informal housing market thrives, as land informality is a subproduct of inefficient and strict regulations. This epistemology makes clear that institutional and regulatory rigidity will not eliminate the demand for housing, as evidenced by the Andalusian Urban Planning Act (LOUA of 2002), which imposed heavy bureaucratic obstacles to prevent the rezoning of rural land (Roy, 2005). On the contrary to what policymakers intended, this restricted formal supply and resulted in more scattered settlements located in rural, peripheral areas (Salvati and Morelli, 2023).

The literature consensus is robust for interpreting the sprawling substitution effect that follows after the relaxation of zoning governance (**Greenaway-McGrevy,** 2023; Murray, 2022). The treated plots for the LISTA law have shown a decrease of -1.2% in their probability for residential sprawl. As theory would suggest and corroborated by **Greenaway-McGrevy (**2023) and **Greenaway-McGrevy (**2023) in their studies in New Zealand, investment decisions channel towards the higher value plots that meet the stricter requirements, as well as their better spatial connectivity and geographical suitability (Wiebe, 2025; Greenaway-Mcgrevy, 2023).

In other words, the LISTA law has incentivized investments towards the larger observations and upzoning them. As their area is above the 2.5 ha legal requirement, it allows for the possibility of legalizing their development (Perujo-Villanueva et al., 2017). This spatial substitution, however, will promote low density development in the existing constructions, unless their development is delineated to their precise perimeter (Serkin and Best, 2023). In essence, the prohibition of dividing agricultural parcels into smaller plots was done for the sole purpose of preventing further urbanization.

Additionally, the Assimilated to the Out-of-Ordinance Regime certificate (AFO) introduced in the LISTA has accentuated this skewed distribution. This certification for demonstrable illegal structures built up before 2016 allowed their legal access to basic services, i.e. electricity, sewage, etc… (Esgaestudio, 2022). The opportunity cost being that these edifications will be legally registered and regularly monitored, as the AFO prohibits the expansion of the building in any way, shape or form, ultimately funnelling development and decreasing the aggregate urban sprawl probability in the region (Serkin and Best, 2023; Esgaestudio, 2022).

2.4 The Physical Intensive Dimension

The Physical Intensive Dimension refers to the three-dimensional modelling and vertical change detection of the informal settlements. These illegal constructions' vertical scale is heavily dependent on the plot's accessibility to roads, intuitively through gravity models, and its geomorphological attributes (Liu et al., 2024).

The spatial attributes displayed in Jaén have made the detection of illegal buildings through satellite images (i.e. the stereo KOMPSAT-3) inaccurate and inadequate (Varol et al., 2019). The pronounced slopes and shade provided by the landforms, in addition to the natural occlusion of the forest cover have catalysed clandestine development under the optical sensors' blindness (Li and Tan, 2020).

Airborne Light Detection and Ranging (LIDAR) is an active remote sensing technology that launches pulses of laser lights that bounce back, allowing for the measurement of the time difference between emitted and returned beams. Ultimately, this data is stored in point cloud files and are mainly employed for Digital Elevation Models (DEM) (Liu et al., 2024). The Digital Surface Model (DSM) is computed after the filtration of certain elements, such as electric poles, trees and other types of vegetation from the DEM. Removing plain land surface from the DSM, in other words subtracting the DEM, the resulting normalized DSM (nDSM) provides information on the maximum altitude of each building with accuracy at the centimeter scale (Varol et al., 2019).

This improved performance is shown in the empirical results of Varol et al. (2019). In this study, LIDAR results were able to detect that 16% of the buildings in the dataset did not comply with the altitude limit requirements, while models from satellite imagery could only detect 1%. The Intersection over Union (IoU) metric shows a 6% increase in overall accuracy of illegal buildings in complex and unconventional environments (Du et al., 2024).

Materials and Logistics assessments on the region have made evident that traditional illegal construction practices on rustic land require a substantial amount of locally sourced non-industrial materials, such as clay, bricks, and others (Mottelson, 2025). The paving of streets has indicated a substantial reduction in transportation costs through the acquisition of motor vehicles, demonstrating a nonlinear relationship with the access to these roads (**Quintas-Soriano, C., Buerkert, A., and Plieninger, T.,** 2022). This lack of infrastructure, combined with the population's lack of access to credit, has frozen the investments into small constructions on the periphery, limiting their vertical and horizontal living area (**Marx, Stoker and Suri, 2013)**.

In the research corpus of the Physical Intensive dimension, a positive relation has been found between the vertical growth of the building and the mean slope of the parcel (Bozzolan et al., 2020; Sidle and Ziegler, 2012; Verniz et al., 2025). This is due to slope cutting in mountainous regions, where vertical separations are made on the soil in order to flatten the ground and allow the construction of households. The reasoning behind this is to avoid the detection by two-dimensional optical sensors, as this will blend the geometry of the building with the vegetation cover (Varol et al., 2019).

On the other hand, Bozzolan et al. (2020) recognizes that these anthropological interactions on the hillside can increase landslide risk during heavy rainfalls up to 85%. This will instigate the property line setbacks and the owner's inability to comply with the State's regulations (Verniz et al., 2025). This was modelled through a

Combined Hydrology and Stability Model (CHASM) that integrates soil filtration and slope stability.

2.5 Research Gap

This thesis focuses on a microanalysis of the regulatory shock that came from the LISTA law. The empirical research done by Greenaway-Mcgrevy and Phillips (2023) is extended to the Mediterranean Basin's rustic land, as well as the implementation of Wiebe's (2025) two-sector model. This research incorporates the land use exclusivity of the consolidated Mediterranean shrub, as established by Ribeiro et al. (2024) and Burgess (2021).

There has been negligible attention placed into investigating the dynamics of climate change and agricultural land abandonment through thermal stress, as the literature's main focus is surrounding the macroeconomic causalities through the Forest Transition framework (Duarte, Jones and Fleskens, 2008; García-Ruiz and Lana-Renault, 2011; Rudel et al., 2005). This thesis incorporates the extensive dimension analysis by including the mean UTCI at the municipal level in the model to assess the loss in effective labour supply (Worklimate 2.0, 2024).

The standard for studying the informal development of rural areas has been through satellite remote sensing images and their three-dimensional incremental analysis (Li and Tan, 2020). On the other hand, LIDAR technology research has mainly been done in dense urban areas, i.e. the favelas in Brazil (Liu et al., 2024; Varol et al., 2019). The model developed in this thesis incorporates the LIDAR point clouds for the examination of the Physical Intensive dimension. The empirical analysis of the associated risk with slope cutting camouflage and the attractiveness of the property's road connectivity (Bozzolan et al, 2021) is taken into consideration in this model as well.

3. Data and Methodology

3.1 Study Area

The study area is limited to the province of Jaén, Spain, which fosters a semiarid Mediterranean climate, with a proclivity for drought conditions, soil loss and extreme thermal stress from sudden heat waves (Gómez et al., 2003). This region has the world's most extensive monoculture around olive orchards, devoting approximately 75% (585,000 ha) of its arable land to this crop alone (Junta de Andalucía, 2024), emerging as the leading olive oil producer (Perujo-Villanueva et al., 2017).

The historical form of production in this region is based on controlled and low density trees, that require regular pruning and soil water management through rigorous pest control. These are structured as smallholdings located on steep slopes (Gómez et al., 2003). Their productivity has experienced a steady decline, accelerating the shrubbing process of the region (Duarte et al., 2008; Perujo-Villanueva et al., 2017; Ribeiro et al., 2024).

3.2 Study Period

The study period pertains to the years 2020 to 2025; excluding 2021 due to the period of transition and implementation of the LISTA, thus resulting in its missing database. This panel structure includes a baseline year not treated, which will allow for the thesis' examination of the agricultural abandonment and land development responses after the LISTA reform (2022-2025), as well as the exclusion of the noise and disruptions from the global COVID pandemic interval.

3.3 Data sources

Included in this subchapter is the detailed recounting of the sources of information utilized for the construction of the model's database. These are classified into the following subdivision: Agricultural, Land administration and demographic records, or on the other hand, Remote sensing, Topographic, and bioclimatic information.

3.3.1 Agricultural, Land administration and demographic records

- Land Use Information System of Spain (SIPNA) 2018,2020,2022,2023 and 2025 geopackages provided by the National Institute of Geography (IGN) and the Geographic Information Centre (CNIG).

  The SIPNA data extracted allowed for the detection and following of the shrubbing percentage in each parcel of rustic land, as well as for discerning the 2020 vegetation cover as a baseline. It contains percentages for each type of vegetation that covers the plot, also identifying active olive groves. It also contains polygons for institutionally protected areas.

- Agricultural Parcel Information System (SIGPAC) 2025 geopackage, provided by the Department and Ministry of Agriculture, Fishing, Water and Rural Development (MAPA)

  This contains the registration of the property boundaries and land use for the last year of the study period. This provided the information to detect the urban sprawl of parcels catalogued in the SIPNA 2022 as abandoned and shrubbing, creating the dichotomous variable for illegal buildings.

- General Directorate for Cadastre and The Property Registry csv provided by the Regional Government of Andalusia

  The information collected in this source is related to physical and legal land attributes. The variables extracted here include the unique identifier, the total area in hectares and the irrigation infrastructure of each parcel (binary 0-1 variable, 1 if existing).

- Official Gazette of the Regional Government of Andalusia (BOJA) Regulations – Law 7/2021 (LISTA Law), published by the Parliament and Regional Government of Andalusia

  The data extracted, in conjunction with land ownership and boundary delimitation layers processed through QGIS, identifies control (0) and treated (1) observations and a dummy variable for the time period, 1 for post-LISTA implementation years, and 0 for 2020.

- Demographic microdata, csv provided by the National Institute of Statistics (INE)

  In order to ascertain Jaén's institutional boundaries and control for the migration tendencies of agricultural workers, the municipal codes and limits, as well as the population growth rates were computed. In turn, the robustness check calculation through standard clustered errors required this information (Abadie et al., 2023).

3.3.2 Agricultural, Land administration and demographic records

- National Aerial Orthophotography Plan (PNOA) LiDAR, LAZ provided by the IGN.

  These virtual point clouds at the 1-meter ground resolution possess three-dimensional coordinates for the CHM to process the maximum and mean height of the illegal construction detected on the plot in meters.

- Digital Terrain Model, 5-meter resolution TIFF sourced from the Institute of Statistics and Cartography of Andalusia (IECA)

  This published model has the mean altitude above sea level in meters and the mean slope in degrees of inclination.

- CORINE Land Cover (CLC) 2018, TIFF provided by the European Environment Agency (EEA) Copernicus Project

  The international standard database for researchers CLC has lower granularity and a 6-year period. Therefore, it has become blind to the microfragmentation and shrub encroachment dynamics observed in Jaén. In chapter 3.6, the detailed data filtration with the CLC database is presented.

- ERA5-Land Reanalysis and the UTCI, TIFF published by Copernicus Climate Change Services and extracted through Google Earth Engine (GEE)

  The UTCI computed for the model was done through the GEE's code environment and is in Celsius' degrees to quantify thermal stress.

- Road Networks and Urban Infrastructure layers, geopackages by IECA and OpenStreetMaps

  These packages contain the line vectors for the different types of roads and the coordinates of the urban structures' nodes in the region. The processing of these datasets through QGIS permitted the measurement in meters of the plot's mean and minimum distance to the nearest highway, as well as urban node. The other variable evaluated from these databases utilized is their Euclidean distance to the closest metropolitan area.

3.4 Variable Selection

In the context of the Shrubbing extense dimension, the plot's shrubbing percentage vegetation cover (i.e. *matorral_pct*) is standardized with respect to its total area for a continuous scale. A natural logarithm is applied to the *matorralización* variable. The dichotomous dependent variable for the Administrative Intensive dimension (*sprawl_bin*) is a Linear Probability Model (LPM) that represents the likelihood of farms located in common rustic land (Serkin and Best, 2023). These parcels were identified as productive orchards in SIPNA 2018, transitioned into passive shrubland in SIPNA 2022 and are registered as an illegal construction in SIGPAC 2025. The subsample of detected active sprawling detailed in chapter 3.6 is used for the last dimension analyzed and computes the vertical scale of clandestine constructions in meters (*chm_max_panel*) (Varol et al., 2019).

The primary independent variable for analyzing the regulatory shock of the reform is the interaction term between the treatment indicator (LISTA_Treat) and the post reform dummy, while treating 2020 as the baseline in order to isolate the causal effect of the change in regulations in the resulting DiD model.

The mean and minimum distance to the nearest concrete highways (*distcarr_mean*, *distcarr_min*) and urban nodes (*disturb_mean*, *disturb_min*), and the Euclidean distance to the nearest metropolitan area (*HubDist*) are included as control variables for the increasing transportation costs friction and accessibility issues of further away plots (Perujo_Villanueva et al., 2017). As previously discussed, higher degree slopes are abandoned with greater frequency as their land's topography impedes the use of higher machinery and increases the exhaustion of the workforce (Duarte et al., 2008), as well as increase their attractiveness to illegal developers as the occlusion from the vegetation cover is higher (Bozzolan et al., 2020). Therefore, the parcel's mean slope in degrees (slp_mean) and the mean altitude in meters (alt_mean) are introduced as controls as well.

Thermal stress on agricultural labour from increasing temperatures and aridity is controlled by the UTCI (*yUTCI_Mun_mean*). This is an exogenous factor that accelerates the field's loss in profitability, therefore, the desertion of agricultural production (Dasgupta et al., 2021). To control homogeneity derived from their accessibility to capital and the fragmentation of the properties found across the olive groves of Jaén, their area in hectares (*area_ha*) (Wiebe, 2025) and the binary variable for irrigation infrastructure (*Irrigated*) are included (Fraga et al, 2021). Lastly, the municipalities' population growth rates (*TasaCrecimiento*) contain the housing markets and demographic pressures of the region (Barbier et al., 2010).

3.5 Data Preparation

The empirical evaluation of the LISTA Law across the three dimensions previously described required the extraction and fusion of spatial data through algorithms, in order to create a panel dataset at the individual parcel level. The variable construction necessary for the thesis' models was done through a Quantum Geographic Information System (QGIS), Google Earth Engine (GEE) and RStudio environment.

3.5.1 SIPNA 2020 as baseline vegetation

To compute the extent of shrubbing encroachment in rustic land in Jaén, the model seeks to isolate exclusively how the LISTA law affected the treated observations. A major structuring and reclassification of the SIPNA datasets occurred between the 2018 and 2020 publications. Therefore, it is not adequate for establishing parallel trends between the treated and control groups pre-reform, as the only year available for the model is 2020. Thus, that year's SIPNA layer was employed to fix an ex-ante LISTA vegetation cover, in order to compute the net Mediterranean shrubland post-reform through the fixed effects model.

3.5.2 SIGPAC: administrative detection of illegal sprawl

The Land Parcel Information System (SIGPAC) geopackages contain the official land use classification codes and the exact legal boundaries of properties. The 2025 dataset was intersected with the SIPNA rustic land layer in a GIS environment in order to partition treated observations that were categorized as developed land in the 2025 census ($LISTA\_Treat_i = 1$). Section 3.6 describes in detail the data filtering procedures executed. The binary indicator for sprawl (*sprawl_bin*$_{i,t}$) is defined as follows:

$$sprawl_{bin_{it}} = \begin{cases} 1\ if\ an\ artifical\ construction\ was\ detected \\ 0\ on\ the\ contrary \end{cases} \tag{3}$$

The post reform time indicator ($Post_t$) is given a value of 0 for 2020 and 1 for all other years examined.

3.5.3 Measuring construction height through LIDAR

The subsample of the observations with institutionally detected urban sprawl indicated the National Topographic Map of Spain MTN50 (1:50,000 scale) cells to download the LAZ files for. The processing of the files and virtual point clouds resulted in the DSM at the 1-meter resolution. The GIS environment's field calculator allowed for the computing of the CHM (or nDSM) through the already available DTM, which isolates the artificial construction's height. This is specified as follows:

$$nDSM_{x,y} = DSM_{x,y} - DTM_{x,y} \tag{4}$$

Afterwards, the computing of the aggregate nDSM pixels contained within the perimeter of the construction. This provided the maximum and mean vertical height of said building in meters.

3.5.4 Topographic and bioclimatic factors

Regarding the thermal stress conditions of each parcel, applying the zonal statistics tool in QGIS determined the altitude and slope, respectively. For the extreme working conditions imposed by climate change, Google Earth Engine was employed to extract and subsequently aggregate the hourly UTCI rasters. The join by location tool in QGIS was used for assigning each plot's yearly mean UTCI at the municipal level.

3.5.5 Other control variables

The mean and minimum distances to paved roads and urban nodes, as well as the Euclidean distance variables were computed for each parcel in a GIS environment, in conjunction with road networks and infrastructure nodes files published by IECA and the urban hub centroids data by OpenStreetMaps. In relation to the latter variable, the tool Distance to nearest hub was used.

The Euclidean distance ($d_{i,H}$) from each parcel (x_i, y_i) to the primary hub for economic activity in the region (xh, yh) is defined as follows:

$$d_{i,H} = \sqrt{(x_i - x_H)^{\,2} + (y_i - y_H)^{\,2}} \qquad (5)$$

3.6 Data filtering

A rigorous approach was conducted for selecting the observations comprising the dataset. In order to isolate the causal effects from the LISTA reform, instead of capturing measurement errors or atypical values due to spatial or structural anomalies, the following approach for filtering and assigning observations into subsamples is detailed:

1. CORINE Land Cover (CLC) 2018 filtering: The CLC 2018 is set as an exogenous macrofilter prior to the LISTA law. Setting the sample 3 years prior to the legal reforms prevents reverse causality caused through the anticipation effect of landowners. The technical constraints regarding the CORINE's Minimum Mapping Unit (MMU) of 25 hectares and 100-meter spatial resolution has obliqued international research into the microfragmentation of properties, the subsequent shrubbing and, potentially, the illegal development of plots. Therefore, this dataset was employed for filtering plots with active olive groves in rustic land through the classification code '223'.

2. Microlevel filtering through SIPNA 2022: Through a GIS environment, the SIPNA layers were intersected and these agriculturally productive plots in

2018 were tracked pre- and post-LISTA implementation. The SIPNA polygons allowed for determining if an observation is on Common Rustic Land and, therefore, belongs to the treatment group.

3. Trimming at 99%: As the focus of this thesis pertains to small-scale olive orchards farms, the exclusion of the highest 1% in relation to the plot's area was necessary as these have different responses and mechanisms of adaptation to the LISTA law. This sample is used for the Extensive and Administrative Intensive Dimension models.
4. Subsample selection for LiDAR detection: The SIGPAC 2025 binary variable created for detecting illegal construction was used for selecting the subsample of active olive groves in 2018 that transitioned into shrubland in 2022 and are now developed in 2025, which implies a medium-term response to the LISTA 2021 implementation. This subsample is used for the Physical Intensive Dimension.
5. Time-balanced panel: Observations that did not have information for these attributes in any of the study years (2020,2022,2023,2024 and 2025) or had corrupted geometries were eliminated from the final dataset of the models.

3.7 Descriptive statistics

Table 1 contains the data and variables of the Extensive and Administrative Intensive Dimensions, which is presented with the intention to easily identify the value ranges, as well as any anomaly or outlier that may be present. After the data filtration process, there are a total of 31,579 plots identified for all the study years analyzed, which resulted in a balanced panel dataset of 157,895 observations. 20,880 (66.12%) of these were located on Common Rustic Land, the remaining 10,699 did not qualify for deregulation by the LISTA law.

Table 1: Descriptive Statistics for Extensive and Administrative Intensive Sample

Variable	N	Mean	sd	min	max
Shrubland Cover (%)	157,895	43.9594	21.3326	0.0000	100.0000
Urban Sprawl	157,895	0.0226	0.1486	0.0000	1.0000
LISTA Treatment	157,895	0.6612	0.4733	0.0000	1.0000
Plot Area (ha)	157,895	0.9601	3.1260	0.1000	195.8398
Mean Elevation (m)	157,895	725.8169	231.7562	164.7684	1656.4311
Mean Slope (°)	157,895	17.1172	9.2505	0.2604	74.6619
Irrigated Plot	157,895	0.0486	0.2150	0.0000	1.0000
Distance to Paved Road (m)	157,895	105.9158	95.4382	0.0000	817.2668
Distance to Urban Structure (m)	157,895	2629.9479	2103.1792	0.0000	29016.5929
Distance to Metropolitan Area (m)	157,895	8566.5945	4888.8247	31.5605	29735.1376
Mean UTCI (°C)	157,895	98.9833	9.7367	65.2422	124.5000
Population Growth Rate (%)	157,895	-10.0088	16.2120	-35.2589	135.4693

Notes: This table presents the number of observations (N), the mean value, the standard deviation (sd), the minimum value (min), and the maximum value (max) for the listed variables.

The zero-values recorded for the distance to paved roads and urban structures are explained by the geometries of a plot colliding or being fragmented by the building's polygon or road network. Analyzing the statistics for the plots' areas provides the justification for trimming the highest 1% of the variable's values, as these properties with atypical sizes behave differently than a small-scale farm in the face of dwindling profitability caused by climate change, regulatory shocks, etc.

The maximum slope recorded of 74.66°, in conjunction with the maximum distances of 29 km to urban structures and metropolitan areas, demonstrates the severe restrictions for heavy machinery and the geographical isolation under which some of these plots operate under. The range for the municipal population growth rate variable (-35.26% to 135.47%) corroborates the diverse abandonment and intermunicipal migration dynamics of the region.

Table 2 records the descriptive statistics pertinent to the detected urban sprawl subsample of the dataset. This reduces to 892 plots that the SIGPAC 2025 flagged as having illicit constructions. The total number of observations for this panel is 4,460.

Table 2: Descriptive Statistics for Physical dimension and LiDAR Sample

Variable	N	Mean	sd	min	max
Maximum Canopy Height (m)	4,460	4.0231	3.9321	-0.1021	27.1015
Mean Canopy Height (m)	4,460	0.5112	0.9499	-1.2269	13.0265
Urban Sprawl	4,460	0.8000	0.4000	0.0000	1.0000
LISTA Treatment	4,460	0.5235	0.4995	0.0000	1.0000
Plot Area (ha)	4,460	1.1347	2.2421	0.1007	24.6971
Mean Elevation (m)	4,460	776.5001	208.5241	181.3290	1470.3915
Mean Slope (°)	4,460	15.7964	8.3921	0.4144	42.8830
Irrigated Plot	4,460	0.0617	0.2406	0.0000	1.0000
Distance to Paved Road (m)	4,460	104.4245	94.7948	0.0000	778.1793
Distance to Urban Structure (m)	4,460	2688.8913	2209.8749	4.0395	11361.6706
Distance to Metropolitan Area (m)	4,460	9913.0642	5200.2583	531.6099	27607.2507
Mean UTCI (°C)	4,460	96.9909	9.8174	65.2422	124.5000
Population Growth Rate (%)	4,460	-11.0321	19.8448	-35.2589	135.4693

Notes: This table presents the number of observations (N), the mean value, the standard deviation (sd), the minimum value (min), and the maximum value (max) for the listed variables.

The subsample increases the average plot size from 0.96 to 1.13 hectares, as well as the altitude from 725.82 to 776.5 meters, which would suggest that illegal urban development is more inclined towards these types of properties. The mean slope suffers a slight decrease from 17.12 to 15.80 degrees. The negative values for both the maximum and minimum canopy height in meters are interpolation errors derived from the CHM model.

The maps displayed below represent the spatial distribution of the samples previously described:

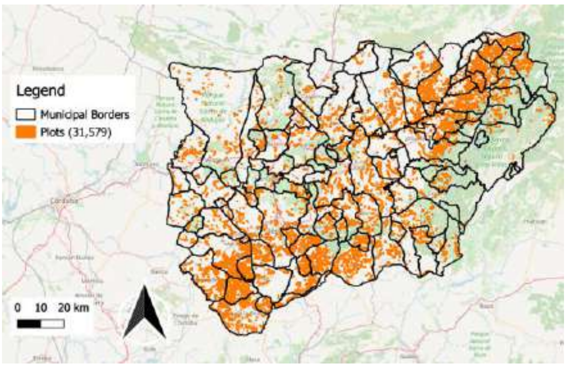

LAYER SOURCES: Municipality borders, INE (2026); Background map, OpenStreetMap.

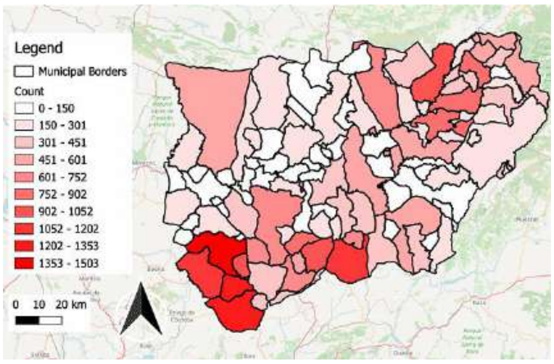

LAYER SOURCES: Municipality borders, INE (2026); Background map, OpenStreetMap.

Figure 1: Spatial distribution of plots in the shrubbing database

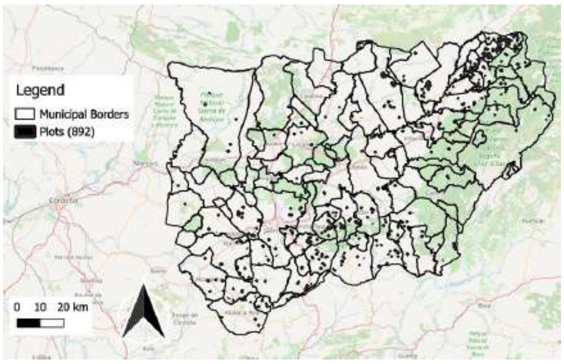

LAYER SOURCES: Municipality borders, INE (2026); Background map, OpenStreetMap.

Figure 2: Distribution of plots per municipality in the shrubbing database

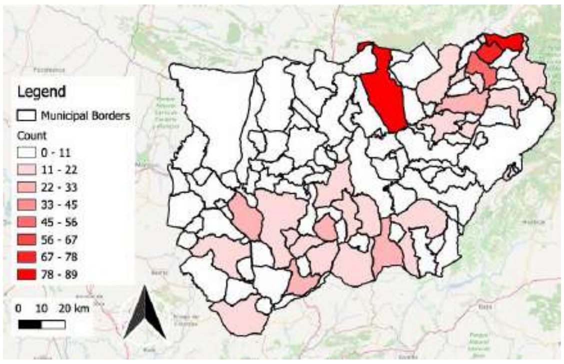

LAYER SOURCES: Municipality borders, INE (2026); Background map, OpenStreetMap.

Figure 3: Spatial distribution of plots in the LiDAR database

Figure 4: Distribution of plots per municipality in the LiDAR database

3.8 Model Choice

3.8.1 Two-way fixed effects

To analyze the LISTA law's effect across all three dimensions, a Two-way Fixed Effects (TWFE) model is optimal in order to control for the main sources of unobserved heterogeneity: time fixed effects (α_i) for macroeconomic shocks and unit fixed effects (λ_t) for individual time-invariant characteristics. For the extensive dimension, the need arises to establish parallel trends between the control and treatment groups pre-reform, thus, an event study specification is preferred for a year-to-year analysis. On the other hand, the DiD static specification is preferred for the physical and administrative intensive dimensions as the sought-after result is the mean (average) effect of the LISTA law on olive groves.

3.8.2 The Linear Probability Model (LPM) and the Administrative Intensive dimension

As the detection of sprawling for the parcels is a binary condition, the LPM model offers distinct utilities in relation to high dimensionality panel data. As such, it will allow for the direct interpretation of the estimated parameters of the model as marginal effects expressed in percentage points. It will also solve the inconsistency and bias issues associated with the use of nonlinear maximum likelihood estimators (i.e., Logit and Probit) (Wooldridge, 2010).

3.8.3 Endogeneity Considerations

The consistency and unbiasedness of OLS estimators rely on certain assumptions, the most important one arguably being that the random error term cannot be related to the regressors (Hanck et al., 2024; Wooldridge, 2010). Legal reforms in relation to land use, infrastructure and transportation needs at this scale are, generally speaking, due to its local demand that pushes policymakers into these decisions (Bento et al., 2003).

In this context, causal simultaneity is mitigated as the LISTA law is a regional level reform, hence the legislative timeline, technical parameters for minimum lot size and the approval process were undisclosed to the individual olive farmers (Ramon y Cajal Abogados, 2025; Greenaway-Mcgrevy and Phillips, 2023; Wiebe, 2025). This indicates that no anticipation effect arose, discarding endogenous selection bias.

Omitted Variable Selection bias is tackled through the fixed effects parameters introduced in the model. Unit fixed effects are used for spatial heterogeneity between plots, such as soil quality, altitude, etc. Time fixed effects are included for considering changes in macroeconomic or climatic variables that have a homogenous effect on observations (Duarte et al., 2008; Wooldridge 2010).

The interaction term between the spatial controls for 2020 and the post-treatment variable ensures no diverging trends between parcels that share geomorphological conditions (Wiebe, 2025; Greenaway-Mcgrevy and Phillips, 2023).

3.8.4 Other OLS assumptions

The second assumption of OLS relates to the independent and identically distributed (i.i.d.) condition for the variables (Hanck et al., 2024). As spatial autocorrelation in the residuals would determine, this assumption does not hold and is circumvented by computing robust standard errors at the municipal level (Conley, 1999; Wooldridge, 2010).

The third assumption calls for outliers rarely being present in the data, which is inaccurate for the severely right-skewed distribution of the maximum building height (CHM) and for the distances to paved roads. A natural logarithm is applied to the continuous variable of this dimension, for ease of interpretability reasons, as well as the need for stabilizing the error’s variance and meeting the assumptions of normality required for inference (Hanck et al., 2024). The transformed distribution of variables that had a natural logarithm applied to them can be observed in the following figures:

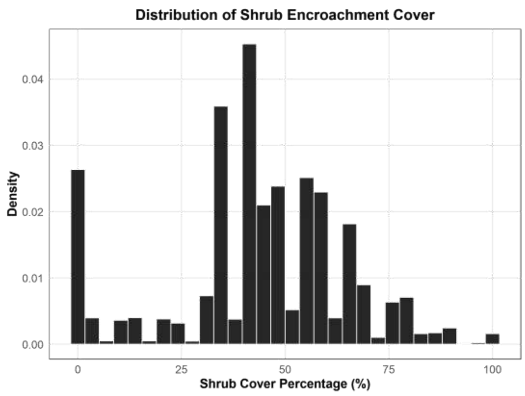

Figure 1: Distribution of Shrub encroachment cover variable

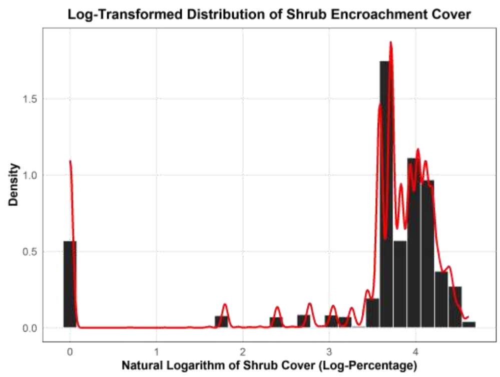

Figure 2: Log-Transformed distribution of Shrub encroachment cover variable

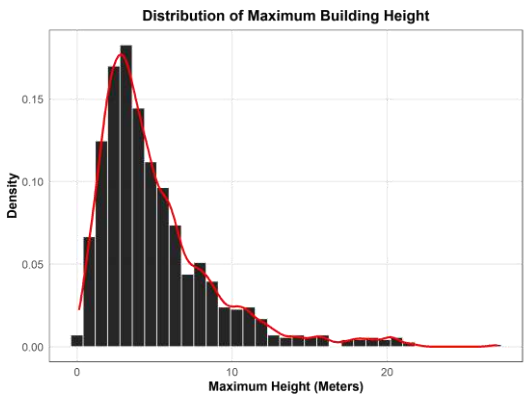

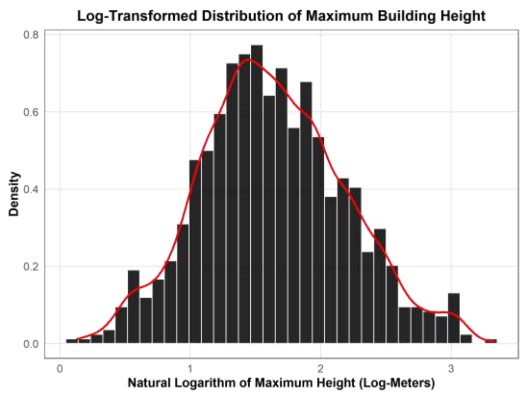

Figure 3: Distribution of maximum CHM variable.

Figure 4: Log-Transformed distribution of maximum CHM variable.

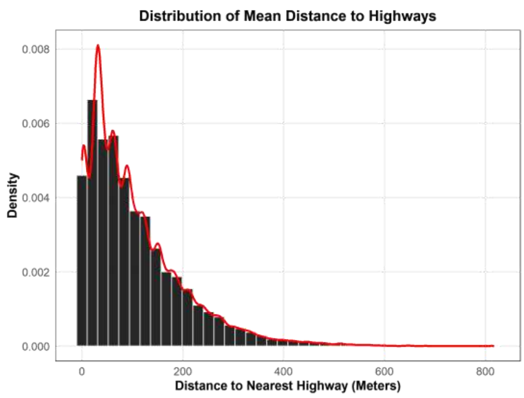

Figure 5: Distribution of mean distance to paved roads variable.

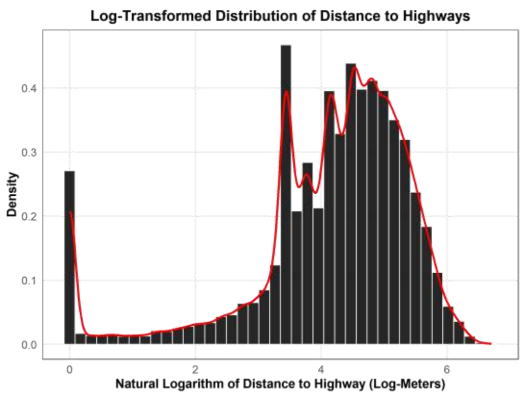

Figure 6: Log-Transformed distribution of mean distance to paved roads variable.

Lastly, no independent variable can be a linear combination of other variables within the model (Hanck et al., 2024). The pairwise comparisons for all variables through Pearson's correlation coefficient present no results that approximate a value of |1|.

3.9 Model specification

3.9.1 Extensive Dimension

The event study with a TWFE model for measuring the percentage of shrub encroachment post-reform is specified as follows:

$$Y_{i,t} = \alpha_i + \lambda_t + \sum_{\tau \neq 2020} \beta_\tau \big(Lista\_Treat_i \text{ x } \mathbb{I}(ano_t = \tau)\big) + \sum_{k} \sum_{t \neq 2020} \gamma_{k,\tau} \left(W_{k,i} \text{ x } \mathbb{I}(ano_t = \tau)\right) + \epsilon_{i,t} \tag{6}$$

where Y is the shrub vegetation (matorral_pct$_{i,t}$) for each plot i on year t, α_i is the plot fixed effects, λ_t is the time fixed effects, $Lista\_Treat_i$ is the dummy variable for treatment, β_τ captures the dynamic effects of each year with the baseline 2020, $W_{k,i}$ is the vector matrix for all time invariant control variables and allows for time flexible trends, and $\epsilon_{i,t}$is the error term clustered at the municipal level.

The interaction term ($Lista\_Treat_i$ x $\mathbb{I}(ano_t = \tau)$ is added for dynamism in the event study and to compute a coefficient for each time period, excluding the baseline year. The second part of the equation is a double summation to allow the fixed spatial controls dynamism across time.

3.9.2 Administrative Intensive Dimension

The discrete probability of illicit urban development is modelled as an LMP model as follows:

$$Y_{i,t} = \alpha_i + \lambda_t + \theta_1(Lista\_Treat_i \text{ x } \mathrm{Post}_t)\sum_k \gamma_k\big(W_{k,i} \text{ x } \mathrm{Post}_t\big) + \epsilon_{i,t} \tag{7}$$

where Y is the binary variable for sprawling (sprawl_bin$_{i,t}$), $Post_t$ is the dichotomous post-reform year indicator, θ_1 is the parameter for measuring the LISTA induced sprawling in percentage points.

3.9.3 Physical Intensive Dimension

The active sprawl subsample is framed through a static DiD, with the TWFE model for measuring the maximum height of structures (*chm_max_panel$_{i,t}$*) outlined below:

$$Y_{i,t} = \alpha_i + \lambda_t + \delta_1(Lista\_Treat_i \text{ x } \mathrm{Post}_t)\sum_k \gamma_k\big(W_{k,i} \text{ x } \mathrm{Post}_t\big) + \epsilon_{i,t} \tag{8}$$

where Y is the altitude in meters and δ_1 is the parameter that isolates and computes LISTA's effect on the vertical change of detected illegal constructions.

4. Results

4.1 Extensive Dimension Model

4.1.1 Regression Results

In table 3, the causal impact of the LISTA Law on shrubbing is estimated through four specifications. An initial finding is that the coefficients for the impact of the reform on treated observations (*LISTA_Treat x Year =*) are all consistently positive and significant when evaluated on the medium-term (2024-2025) across all the models, except for the 2024 coefficient on the baseline specification (Model 1), which is likely due to the exclusion of unit fixed effects that severely underestimates the regulatory shock. While the coefficients for the immediate post-reform year (2022) are highly significant and negative on the first three models, the final specification addresses this reducing their value ≈0 and attaining insignificancy.

Model 1 only includes the interaction term for each year, introduced as a naïve model and reflected by the 42.30 constant in which OLS is attributing most shrubbing to unobservable characteristics. Model 2 is comprised only of the fixed effects for both, units and years. Model 3 includes all socio-demographic and spatial controls. Lastly, Model 4 clusters errors at the municipal level. The LISTA law has increased shrubbing in rustic land in Jaén in 1.2 percentage points. A graphical representation of these findings is displayed in figure 7.

Acknowledging goodness of fit, all fixed effects specifications estimate that approximately 57.55% of the variation of land abandonment is explained through the inherent fixed heterogeneity of the plot (geography, accessibility, etc…). The R^2 *Within* significantly improves between the second and final specification, rounding up to a 0.006 value in model 4. This substantiates the dynamic geomorphological controls included in the model.

The full estimated results are available in the first table of the Appendix. Concerning the control variables at the municipal level, Model 3's population growth rate has negative and significant coefficients for the years 2022, 2024 and 2025 (-0.0314, -0.0244 and -0.0242, respectively). While 2025's coefficient is not significant in the final specification, the increasingly negative growth rates have accelerated the

abandonment of olive orchards and, therefore, has enabled the onslaught of shrubland in Jaén at the medium term.
On a similar note, thermal stress coefficients also indicate to have advanced Jaén's shrub colonization. In 2022, the coefficient is computed as extremely significant and positive (0.0948) but turns insignificant and decreases in Model 4 (0.0386). This stems from the introduction of errors clustered at the municipal level, as this will absorb most of the bioclimatic variable.
Analysing the plot's individual-level control variables, the parcel's area coefficient in 2022 for Model 4 is highly significant and positive. For every additional hectare, the shrubbing increased 37%. This specification estimated significant and negative values for the farm's altitude in 2023 and 2024 (-0.0042 and -0.0030, respectively). This implies that in 2023, for every additional 100 meters to the Y geocoordinate of a plot, its shrubbing was 0.42% less when in comparison to the lower altitude one.
Lastly, when analysing the accessibility control variables in the final specification, it is evident that the mean distance to urban structures is the most determinant factor for the immediate years post LISTA implementation. In 2022, for every additional 1,000 meters in this average, shrubbing increased 0.70%. Successively, the parcel's mean distance to paved roads has a positive and significant coefficient for 2024 and 2025, pointing towards a 0.4 percentage points increase for every 100 added meters in this parameter.

Table 3: Impact of the LISTA Law on Shrubland Cover

	Model 1 (OLS)	Model 2 (Pure TWFE)	Model 3 (+ Mun. Controls)	Model 4 (Final Spec.)
Dependent Variable:	Shrubland Cover (%)			
LISTA_Treat × Year = 2022	9.223^{***}	-1.155^{***}	-1.495^{***}	-0.6451
	(0.1654)	(0.3138)	(0.3328)	(0.6580)
LISTA_Treat × Year = 2023	2.005^{***}	0.0365	-0.0221	0.0590
	(0.1654)	(0.3485)	(0.3755)	(0.6666)
LISTA_Treat × Year = 2024	0.2475	1.334^{***}	1.646^{***}	1.216^{*}
	(0.1654)	(0.3577)	(0.3792)	(0.6544)
LISTA_Treat × Year = 2025	1.051^{***}	1.225^{***}	1.351^{***}	1.202^{*}
	(0.1654)	(0.3540)	(0.3793)	(0.6522)
Fixed Effects				
Plot FE (id_0)	No	Yes	Yes	Yes
Year FE (ano)	No	Yes	Yes	Yes
Fit Statistics				
Standard Errors (S.E.)	IID	Clustered (id_0)	Clustered (id_0)	Clustered (id_ine)
Observations	157,895	157,895	157,895	157,895
R^2	0.02020	0.57549	0.57586	0.57766
Within R^2	—	0.00097	0.00185	0.00609

Notes: The dependent variable is `matorral_pct` (expressed as a percentage). Standard errors are reported in parentheses below the estimated coefficients. Significance codes: *** $p < 0.01$, ** $p < 0.05$, * $p < 0.1$.

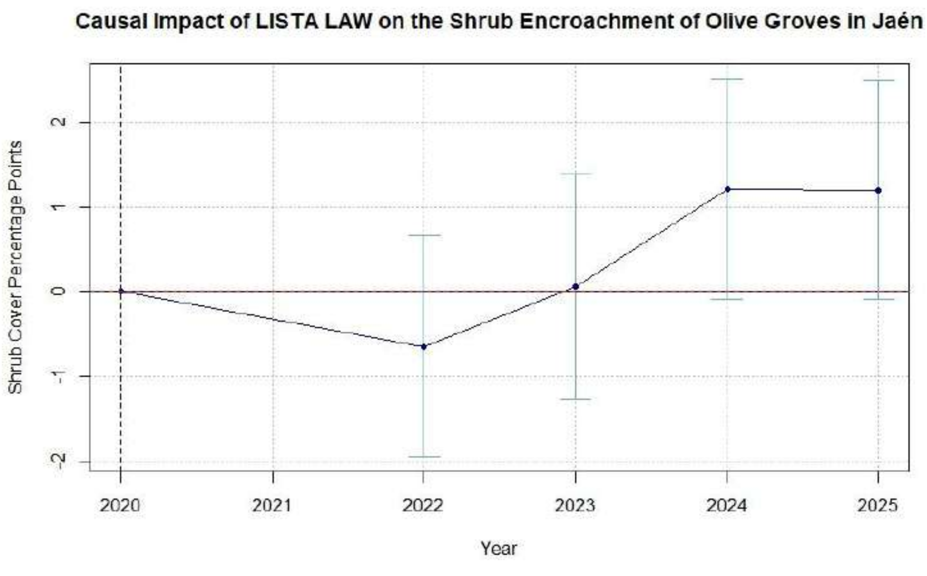

Figure 7: Causal impact of the LISTA reform on the shrub encroachment (%) of Olive Groves in Jaén 2020-2025.

4.1.2 Robustness Checks

In order to estimate the effect of the LISTA law deregulatory shock on the shrubbing of active olive groves, the pertinent study sample was obtained through a specific research design. In this section, five robustness checks are performed to assess the validity of the estimated results. Only the interaction term is examined, as it is the variable of interest. Table 4 displays the results for all five models. Table A2 in the appendix shows robustness checks results for all control variables.

As stated previously, a methodological concern is that larger estates have different adaptation strategies to climate change, access to heavy machinery, among many others, which results in traditional olive orchards in Jaén having different land abandonment dynamics than these properties. Therefore, the first robustness check performed is the trimming of the 1% outliers to the right of the distribution (Column 2). In the same vein, Column 4 refers to the spatial jackknife, where the municipality with the most observations of the dataset (Martos) is excluded. Only the medium-term coefficient of 2024 did not remain significant on the Jackknife, while 2025 and both coefficients of Column 2 remain significant and around the 1.2 value.

The clustering of the standard errors at the municipal level is reasonable given that the reform's treatment varies by the protected status of rustic land. Column 3 displays the coefficients where the errors are clustered at the plot level. The medium-term coefficients are confident at the 90% level in the most restrictive specification (M4), while their significance level is at the 99% level in this robustness check. As land abandonment could be motivated by accessibility efficiency (mean distance) or the minimum distance to paved roads, these are included as variables in Column 5 and in Column 6 nonlinear quadratic terms for the area, slope and altitude of the plot are introduced. In these last two, both medium-term coefficients for the variable of interest remained significant at the 90 % confidence level and a ≈1.2 value (1.258 and 1.219, respectively).

Table 4: Robustness Checks for Extensive dimension model

	(1) Baseline (M4)	(2) Excl. Large Estates	(3) Plot Cluster	(4) Geog. Exclusion	(5) Min. Distances	(6) Nonlinear Form
Dependent Variable:	Shrubland Cover (%)					
LISTA_Treat × Year = 2022	-0.6451	-0.2894	-0.6451*	-0.6409	-0.6474	-0.3697
	(0.6580)	(0.6487)	(0.3463)	(0.6853)	(0.6584)	(0.6422)
LISTA_Treat × Year = 2023	0.0590	0.0185	0.0590	0.0557	0.0648	0.0630
	(0.6666)	(0.6702)	(0.3881)	(0.7017)	(0.6666)	(0.6692)
LISTA_Treat × Year = 2024	1.216*	1.163*	1.216***	1.124	1.226*	1.258*
	(0.6544)	(0.6647)	(0.3934)	(0.6781)	(0.6546)	(0.6631)
LISTA_Treat × Year = 2025	1.202*	1.118*	1.202***	1.301*	1.218*	1.219*
	(0.6522)	(0.6471)	(0.3865)	(0.6734)	(0.6512)	(0.6318)
Fixed Effects						
Plot FE (id_0)	Yes	Yes	Yes	Yes	Yes	Yes
Year FE (ano)	Yes	Yes	Yes	Yes	Yes	Yes
Fit Statistics						
S.E. Cluster	id_ine	id_ine	id_0	id_ine	id_ine	id_ine
Observations	157,895	156,315	157,895	150,380	157,895	157,895
R^2	0.57766	0.57998	0.57766	0.57591	0.57764	0.57861
Within R^2	0.00609	0.00748	0.00609	0.00635	0.00605	0.00832

Notes: This table presents robustness checks for the baseline specification (Model 4). Column (2) excludes large estates to account for outliers. Column (3) clusters standard errors at the plot level. Column (4) implements geographic exclusion criteria. Column (5) controls for minimum distances, and Column (6) estimates a non-linear functional form. Standard errors are in parentheses. Significance: *** $p < 0.01$, ** $p < 0.05$, * $p < 0.1$.

4.2 Administrative Intensive Model

In table 5, the coefficients relating to the probability of illegal urban development on rustic shrubbing land are displayed. Column 1 presents the LPM specification, which alludes to a 1.22 percentage point reduction in Jaén's common rustic land plots probability to have been unlawfully developed since their deregulation through LISTA in 2021. Only two of the control variables resulted in significant coefficients, the individual plot's average slope and distance to regional urban hub and were significant at the 90% level. The former's negative value is 0.00039 and states that for every additional 10° on the average slope of a treated plot, a 0.39% decrease was experie4nced in their probability of being illicitly developed. On the other hand, the latter has been attributed a positive value interpreted as an increase of 0.124% in the plot's probability of having had an illegal structure erected on their perimeter post-reform, for every additional 1,000 meters away from the nearest regional urban hub.

Turning the analysis to goodness of fit, the model explains 80.22% of the unlawful structures, which is to be expected as a plot's condition of being constructed upon or not is majorly determined by the inherent geographical characteristics. The modest 0.00530 value of the R^2_{Within}, is predictable from the class imbalance in the dataset.

The robustness checks performed for this dimension's model are reported in this table, as well. Clustering at the municipal level, the standard errors of the model were reduced in more than half from 0.00760 to 0.00261. Consequently, the already significant values are now so at the 99% confidence interval, and the dependent variable and four other control variables are now highly significant. For every additional degree of the municipal's UTCI average, there is an additional 0.031 percentage points for sprawl. The presence of irrigation structure and the plot's altitude have a positive relationship with illegal development. If marked with irrigation, the plot has an additional 0.803% probability to have been developed post-LISTA. The addition of 100 units to the *y* geocoordinate of the plot resulted in an increase of 0.127% on their probability of sprawl.

The exclusion of the municipality with the highest observations (Column 3), turned the Distance to Urban Hub coefficient insignificant and reduced it, while the mean slope remains constant. R^2 also remained constant and R^2_{Within} suffered a 3.9% decrease. Lastly, Column 4 presents the robustness check where the minimum distances to highways and urban structures replace their respective averages. The parameters remained constant for this last test. The control variables for growth rate and the parcel's area computed insignificant coefficients throughout all different specifications.

Table 5: LISTA Law Effects on Sprawl Probability

	(1) Baseline (LPM)	(2) Plot Cluster	(3) Geog. Exclusion	(4) Min. Distances
Dependent Variable:	sprawl_bin	sprawl_bin	sprawl_bin	sprawl_bin
LISTA_Treat × Post	-0.01223	-0.01223***	-0.01289	-0.01221
	(0.00760)	(0.00261)	(0.00793)	(0.00758)
Post × Heat Stress (UTCI)	-0.00031	-0.00031**	-0.00025	-0.00031
	(0.00047)	(0.00014)	(0.00047)	(0.00047)
Post × Growth Rate	0.00012	0.00012	0.00015	0.00012
	(0.00015)	(9.33e-5)	(0.00015)	(0.00015)
Post × Area (ha)	0.00027	0.00027	0.00022	0.00028
	(0.00058)	(0.00032)	(0.00057)	(0.00058)
Post × Mean Altitude	1.27e-5	1.27e-5**	1.41e-5	1.28e-5
	(1.56e-5)	(6.1e-6)	(1.63e-5)	(1.56e-5)
Post × Mean Slope	-0.00039*	-0.00039***	-0.00039*	-0.00039*
	(0.00021)	(7.97e-5)	(0.00022)	(0.00021)
Post × Irrigated	0.00803	0.00803**	0.00770	0.00812
	(0.00518)	(0.00349)	(0.00521)	(0.00519)
Distance Interactions				
Post × Mean Dist. to Urban	-6.67e-8	-6.67e-8	-1.02e-7	—
	(2.26e-6)	(5.66e-7)	(2.3e-6)	
Post × Mean Dist. to Roads	6.34e-6	6.34e-6	7.65e-6	—
	(1.13e-5)	(9.54e-6)	(1.19e-5)	
Post × Dist. to Hub	1.24e-6*	1.24e-6***	1.18e-6	1.24e-6*
	(7.34e-7)	(2.61e-7)	(7.4e-7)	(7.31e-7)
Post × Min. Dist. to Urban	—	—	—	-2.28e-8
				(2.26e-6)
Post × Min. Dist. to Roads	—	—	—	1.41e-5
				(1.21e-5)
Fixed Effects				
Plot FE (id_0)	Yes	Yes	Yes	Yes
Year FE (ano)	Yes	Yes	Yes	Yes
Fit Statistics				
S.E. Cluster	id_ine	id_0	id_ine	id_ine
Observations	157,895	157,895	150,380	157,895
R^2	0.80221	0.80221	0.80221	0.80222
Within R^2	0.00530	0.00530	0.00509	0.00535

Notes: This table presents difference-in-differences estimates for the probability of urban sprawl using a Linear Probability Model (LPM). The dependent variable sprawl_bin is a binary indicator (1 = sprawl). Time-invariant biophysical and spatial covariates are interacted with the *Post* indicator. Standard errors are clustered as indicated and reported in parentheses. Significance codes: *** $p < 0.01$, ** $p < 0.05$, * $p < 0.1$.

4.3 Physical Intensive Dimension

The final dimension of analysis refers to the vertical growth reached of illegal constructions detected in Jaén's abandoned plots. The results of the model are presented in table 6. The first column refers to the baseline model, where it starts to become evident that the LISTA reform did not have an effect on the vertical expansion of illegal buildings. The interaction term between the LISTA treatment and the post-reform year is insignificant and has a value of 0.44, indicating that the physical scale of these constructions has no causal relationship with the regulations of land use. The municipal controls coefficients, heat stress and the population's growth rate, are significant and demonstrate negative relationships with the dependent variable (-0.0436 and -0.0116, respectively).

In relation to the plot's individual characteristics, the mean slope coefficient is highly significant and indicates that for every 10 ° increase in the inclination, the structure's maximum height increases by 1.14 meters. A possible explanation for this preference of illegal developers is that the more pronounced gradient provides natural vegetation cover for the building's structure (Varol et al., 2019). The cost of transport and heavy machinery still has influence in their decision, as captured by the distance to urban hub coefficient; for every 1,000 meters the plot is further away, the maximum height is reduced by 8.67 centimeters. In the same vein as last model, evaluating the R^2 demonstrates that ≈80% of the variability is dependent on the plot's individual characteristics. The model's high explanatory capacity at the intra-plot level is displayed by the R^2_{Within}=0.07083.

The validity of these results is tested through three robustness checks. The first of these is performed by substituting the dependent variable of maximum CHM, to the minimum CHM in meters. The LISTA term remains insignificant, while the slope remains and establishes itself as the predominant factor. One thing to note is that the plot's area coefficient turns negative with a value of 0.0188 significant at the 90% confidence level. This estimates a decrease of 1.88 centimeters on the dependent variable for every additional hectare on the plot's total size. A possible mechanism behind this is that smaller properties must use efficiently their limited space, sprawling vertically. On the other hand, larger properties can afford the space to sprawl horizontally within their property, reducing the total average.

The second test limits the maximum height of structures distribution at the 98% level, discarding outliers (values reached up to 27.10 meters). There is a notable reduction in the standard error compared to the baseline model (0.3702 to 0.2658) and this in turn validates the insignificance of the reform in relation to the dependent variable. Goodness of fit improves to R^2=0.79894, while R^2_{Within} remains ≈0.07. The negative population growth rates of Jaén point towards less supervision and governmental enforcement and, thus, higher incentives to build taller. The plot's mean altitude turns significant at the 95% confidence level and with a positive value of 0.0021 confirms that the vertical growth of clandestine structures is not related to regulation, but instead to the plot's geographical advantages. In this case, the higher altitude of the plot gives a relative higher altitude to the structure compared to the vegetation cover downhill, thus, a scenic view.

Table 6: LISTA Law Effects on Vertical Growth of Illegal Buildings

	(1) Baseline (Max CHM)	(2) Mean Height (Mean CHM)	(3) Trimmed 98%	(4) Min. Distances
Dependent Variable:	chm_max_panel	chm_mean_panel	chm_max_panel	chm_max_panel
LISTA_Treat × Post	0.4466	0.0366	0.2971	0.4719
	(0.3702)	(0.1143)	(0.2658)	(0.3703)
Post × Heat Stress (UTCI)	-0.0436**	-0.0221***	-0.0150	-0.0429**
	(0.0215)	(0.0064)	(0.0180)	(0.0214)
Post × Growth Rate	-0.0116*	-0.0014	-0.0103**	-0.0126**
	(0.0064)	(0.0030)	(0.0049)	(0.0060)
Post × Area (ha)	0.0389	-0.0188*	0.0557	0.0347
	(0.0508)	(0.0110)	(0.0516)	(0.0505)
Post × Mean Altitude	0.0014	0.0004	0.0021**	0.0014
	(0.0011)	(0.0004)	(0.0009)	(0.0012)
Post × Mean Slope	0.1141***	0.0165**	0.0807***	0.1122***
	(0.0242)	(0.0071)	(0.0150)	(0.0242)
Post × Irrigated	-0.4162	0.1825	-0.1110	-0.3821
	(0.4989)	(0.2920)	(0.4917)	(0.5048)
Distance Interactions				
Post × Mean Dist. to Urban	9.97e-5	2.25e-5	7.16e-5	—
	(0.0001)	(2.54e-5)	(0.0001)	
Post × Mean Dist. to Roads	-0.0014	-0.0002	-0.0013	—
	(0.0013)	(0.0004)	(0.0013)	
Post × Dist. to Hub	-8.67e-5**	-3.4e-6	-7.14e-5**	-9.00e-5**
	(4.12e-5)	(1.24e-5)	(3.09e-5)	(4.21e-5)
Post × Min. Dist. to Urban	—	—	—	9.85e-5
				(0.0001)
Post × Min. Dist. to Roads	—	—	—	-0.0043**
				(0.0020)
Fixed Effects				
Plot FE (id_0)	Yes	Yes	Yes	Yes
Year FE (ano)	Yes	Yes	Yes	Yes
Fit Statistics				
S.E. Cluster	id_ine	id_ine	id_ine	id_ine
Observations	4,460	4,460	4,388	4,460
R^2	0.78257	0.67191	0.79894	0.78403
Within R^2	0.07083	0.04697	0.06556	0.07711

Notes: This table presents difference-in-differences estimates for vertical growth using Canopy Height Models (CHM) derived from LiDAR data. Time-invariant biophysical and spatial covariates, including Heat Stress (UTCI), are interacted with the *Post* indicator. Standard errors are clustered at the municipal level (id_ine) and reported in parentheses. Significance codes: *** $p < 0.01$, ** $p < 0.05$, * $p < 0.1$.

5. Conclusion and Discussion

5.1 Conclusions

This thesis' aim was to answer the following primary research question: "**To what extent did the relaxation of regulations of rustic land through the LISTA law causally affect the agricultural land abandonment and illegal urban sprawl in Jaén, Spain?**". To this effect, a panel dataset composed of 31,579 parcels was constructed using LiDAR data, GIS-software and analyzed in an R-environment through three different dimensions: Extensive, Administrative Intensive and Physical Intensive. Following Navarro et al. (2023) and Wiebe's (2025) two-sector model, the shrubbing, presence of illicit buildings on parcels and CHM model of the subsample were examined through two-way fixed effects and linear probability models.

Firstly, land abandonment and the ensuing shrubbing (Extensive dimension) were analyzed and the LISTA law had a positive and significant effect on the shrub percentage of the plot's vegetation cover. In 2024-2025, 1.216 and 1.202 percentage points, respectively. However, on the least conservative specification (standard errors clustered at the municipal level) the coefficient reached 1.646%. These results were put through five different robustness checks, which confirmed the consistency of the parameters estimated.

The second dimension analyzed was the Administrative Intensive, in which the LPM model computed a significant and negative coefficient of 0.01223 in relation to the treated plot's probability of detected illegal urban sprawl post-reform. The results were significant at the 99% confident level when using clustered level standard errors specification, and there was negligible variation in the parameters when put through the spatial Jackknife test and minimum distances variable substitution.

The Physical Intensive Dimension model analyzed the subsample and estimated a statistically insignificant value of 0.4466 meters ($p = 0.228$), thus the vertical growth of illegal structures does not respond to regulations and institutional intervention. Instead, the accessibility and geographical advantages of a plot's location have proven to be the most determinant factors of unlawful urban development.

5.2 Interpretation of results

The difference in shrubbing between the treated and control groups confirmed that the flexibilization of the requirements for building on the former resulted in the cost of opportunity changing and increased incentives for the abandonment of olive groves on the verge of profitability. In particular, the ever-decreasing population growth rates and increase in thermal stress through climate change variables confirmed that the sharp decline experienced in the worker's capacity and agricultural labor supply has intensified the abandonment of steeper sloped parcels.

Similarly, as in **Greenaway-McGrevy (**2023), the model computed for the Administrative Intensive analysis corroborated that investment of illegal urban developers was funneled, as analyzed in **Greenaway-McGrevy (**2023), towards already constructed buildings built before 2015. In essence, the probability of urban sprawl on LISTA treated plots was reduced by 1.22 percentage points, where the presence of irrigation infrastructure and the further away the plot is from metropolitan areas is preferred.

The CHM analysis for the illegal constructions detected in the dataset revealed that their vertical growth does not depend upon their institutional framework, as their main preferences hinge upon the geographical conditions that allow for natural amenities and camouflage of the building's geometry through the vegetation cover against satellite detection (Varol et al., 2019). For each additional 10° of the plot's mean slope, there is a 0.1441 meter increase in the construction's height. The accessibility of the plot to paved roads, as well as their distance to the nearest urban hub impose transportation costs and are determinants towards the vertical height of unlawful constructions as well.

5.3 Limitations

One technical limitation is related to the availability of yearly LiDAR 3D data in order to produce a time-series analysis of vertical growth, as the results from this thesis assumed a zero-value of meters at the baseline year of analysis and this impedes the continuous evaluation of the construction's height. Another limitation of this study is the computing of Euclidean distances for all variables relating to the plot's accessibility variables. In Jaén's mountainous context, this is an oversimplification of the geomorphology and could be a source of bias.

The LiDAR LAZ files for the full dataset were computationally demanding and impeded the model's estimation, therefore the subsample where SIGPAC 2025 detected sprawling was preferred.

The farm's individual cost structure and unit-level data, as well as the price of olive oil in the region could be a source of unobserved heterogeneity and their inclusion should be further explored. The external validity of these results is limited as they are representative of the traditional olive monoculture of Jaén.

5.4 Further Research

The following are possible avenues for further research derived from the study's conclusions and limitations. Further research could use the full dataset in conjunction with the LiDAR data for all observations instead of limiting the model's design to only observations contained in the subsample. Another extension could be evaluating if the substitution effect ("funneling") of the illegal housing market occurred by obtaining the municipal AFO licenses requests.

6. References

Abadie, A., Athey, S., Imbens, G. W., & Wooldridge, J. M. (2023). When should you cluster standard errors? *Econometrica*, 91(1), 1–35.

Alonso, W. (1964). Location and Land Use: Toward a General Theory of Land Rent. Harvard University Press.

Autonomous Community of Andalusia. (2021). *Law 7/2021, of December 1, for the Promotion of Territorial Sustainability in Andalusia (LISTA)* [Ley 7/2021, de 1 de diciembre, de Impulso para la Sostenibilidad del Territorio de Andalucía]. *Official Gazette of the Regional Government of Andalusia (BOJA)*, 233, 1–118.

Barbier, E. B., Burgess, J. C., & Grainger, A. (2010). The forest transition: Towards a more comprehensive theoretical framework. *Land Use Policy*, *27*, 98–107. https://doi.org/10.1016/j.landusepol.2009.02.001

Baudena, M., Santana, V. M., Baeza, M. J., Bautista, S., Eppinga, M. B., Hemerik, L., ... & Rietkerk, M. G. (2020). Increased aridity drives post-fire recovery of Mediterranean forests towards open shrublands. *New Phytologist*, 225(4), 1500–1515. https://doi.org/10.1111/nph.16252

Bento, A. M., Cropper, M. L., Mobarak, A. M., & Vinha, K. (2003). The impact of urban spatial structure on travel demand in the United States (Policy Research Working Paper No. 3115). The World Bank.

BOE. (2021). Ley 7/2021, de 1 de diciembre, de impulso para la sostenibilidad del territorio de Andalucía. *Boletín Oficial del Estado*, num. 294, de 9 de diciembre de 2021. https://www.boe.es/buscar/act.php?id=BOE-A-2021-20916

Bozzolan, E., Holcombe, E., Pianosi, F., & Wagener, T. (2020). Including informal housing in slope stability analysis – an application to a data-scarce location in the humid tropics. *Natural Hazards and Earth System Sciences*, 20(11), 3161–3179. https://doi.org/10.5194/nhess-20-3161-2020

Burgess, P. (2021). *Wildfire risk can be reduced with agroforestry*. Cranfield University / PreventionWeb. https://www.preventionweb.net/news/wildfire-risk-can-be-reduced-agroforestry

Carmona-Torres, C., Parra-López, C., Sayadi, S., & Reina-Usuga, L. (2023). Abandonment factors and alternatives in sloping olive growing: The case of Andalusia, Spain. Land Use Policy, 132, Article 106836. https://doi.org/10.1016/j.landusepol.2023.106836

Conley, T. G. (1999). GMM estimation with cross sectional dependence. *Journal of Econometrics*, 92(1), 1–45.

Copernicus Climate Change Service. (2025). *ERA5-Land reanalysis data and Universal Thermal Climate Index (UTCI)* [Spatial raster dataset]. European Centre for Medium-Range Weather Forecasts (ECMWF) / Google Earth Engine Catalog.

Coppola, P. (2022). The plurality of urban informal practices: connections with public institutions in Italy. *Urban Studies*, 59(12), 2411–2430.

Črepinšek, Z., Žnidaršič, Z., & Pogačar, T. (2023). Spatio-Temporal Analysis of the Universal Thermal Climate Index (UTCI) for the Summertime in the Period 2000–2021 in Slovenia: The Implication of Heat Stress for Agricultural Workers. *Agronomy*, 13(2), 331. https://doi.org/10.3390/agronomy13020331

Dasgupta, S., Robinson, E. J. Z., Shayegh, S., Bosello, F., Park, R. J., & Gosling, S. N. (2024). Heat stress and the labour force. *Nature Reviews Earth & Environment*, 5(12), 859–872.

Du, J., Fan, C. L., & Ji, S. (2024). An optimized edge-focused Siamese network for monitoring new illegal buildings using satellite images. *IEEE Transactions on Geoscience and Remote Sensing*, 62, 1–15.

Duarte, F., Jones, N., & Fleskens, L. (2008). Traditional olive orchards on sloping land: Sustainability or abandonment? *Journal of Environmental Management*, 89(2), 86–98.

Esgaestudio. (2022). *¿Qué es la asimilación fuera de ordenación (AFO)?* Esgaestudio de Arquitectura e Ingeniería.

European Environment Agency. (2018). *CORINE Land Cover (CLC) 2018* [Raster spatial dataset]. Copernicus Land Monitoring Service.

FAO. (2020). *Working in a hot environment: Manual on occupational safety and health*. Organización de las Naciones Unidas para la Alimentación y la Agricultura (FAO). Roma, Italia.

Fraga, H., Pintar, M., & Pinto, R. (2021). Mediterranean Olive Orchards under Climate Change: A Review of Future Impacts and Adaptation Strategies. *Agronomy*, 11(1), 56.

García-Ruiz, J. M., & Lana-Renault, N. (2011). Hydrological and erosive consequences of farmland abandonment in Europe, with special reference to the Mediterranean region - A review. *Agriculture, Ecosystems and Environment*, *140*, 317–338.

General Directorate for Cadastre. (2025). *Cadastral cartography and microdata for the Province of Jaén* [Spatial and alphanumeric dataset]. Ministry of Finance and Public Function of Spain.

Gómez, J. A., Battany, M., Renschler, C. S., & Fereres, E. (2003). Evaluating the impact of soil management on soil loss in olive orchards. *Soil Use and Management*, 19(2), 127-134.

Greenaway-McGrevy, R. (2023). *The impact of widespread upzoning on housing construction: Evidence from Lower Hutt* (Working Paper No. 18). Business School, University of Auckland.

Greenaway-McGrevy, R., & Phillips, P. C. B. (2023). The impact of upzoning on house construction and rents: New Zealand evidence. *Journal of Urban Economics*, 136, 103573.

Gual Suárez, Gianlorenzo (2024). Valor implícito de la lluvia y la temperatura en la producción de maíz grano en México durante el periodo 2003-2021. [Bachelor Thesis]. Facultad de Economía, UNAM. https://repositorio.unam.mx/contenidos/3726193

Hanck, C., Arnold, M., Gerber, C., & Schmelzer, M. (2024). *Introduction to Econometrics with R*. University of Duisburg-Essen. https://www.econometrics-with-r.org/

ILO. (2019). *Working on a warmer planet: The impact of heat stress on labour productivity and decent work*. Oficina Internacional del Trabajo (OIT). Ginebra, Suiza.

Institute of Statistics and Cartography of Andalusia. (2025a). *Digital Terrain Model of Andalusia: Altitudes and Slopes (DTM 5m)* [Raster spatial dataset]. Regional Government of Andalusia.

Institute of Statistics and Cartography of Andalusia. (2025b). *Road networks and urban infrastructure of Andalusia* [Vector spatial dataset]. Regional Government of Andalusia.

Junta de Andalucía. (2024). *Balance del trabajo que realizan las nueve Oficinas Comarcales Agrarias (OCA) de la provincia de Jaén para seguir ofreciendo un servicio eficaz a los 97 municipios de la provincia*. Consejería de Agricultura, Pesca, Agua y Desarrollo Rural

Li, B. S., & Tan, Z. C. (2020). Dynamic monitoring method of illegal buildings using spatiotemporal big data based on urban high lying zones. *Transactions in GIS*, 24(1), 88–104.

Liu, C., Jang, K. M., Dimitrov, S., Ferreira Barbalho, C. L., Duarte, F., & Ratti, C. (2024). Unveiling the internal structures of informal settlements through AI-driven automated segmentation of LiDAR data. *npj Urban Sustainability*, 4(1), 12.

Marx, Benjamin, Thomas Stoker, and Tavneet Suri. 2013. "The Economics of Slums in the Developing World." Journal of Economic Perspectives 27 (4): 187–210

Ministry of Agriculture, Fisheries and Food. (2025). Geographic Information System of Agricultural Parcels (SIGPAC) 2025 [Geopackage]. Regional Ministry of Agriculture, Fisheries, Water and Rural Development of Andalusia.

Moreira, F., Ascoli, D., Safford, H., Adams, M. A., Moreno, J. M., Pereira, J. M. C., Catry, F. X., Armesto, J., Bond, W., González, M. E., Curt, T., Koutsias, N., McCaw, L., Price, O., Pausas, J. G., Rigolot, E., Stephens, S., Tavşanoğlu, Ç., Vallejo, V. R., ... Fernandes, P. M. (2020). Wildfire management in Mediterranean-type regions: Paradigm change needed. Environmental Research Letters, 15(1), 011001

Mottelson, J. *(2025). Modern Vernacular: Informal Housing Architecture and Urban Resilience. En Resilient Urbanism (pp. 35–55). Routledge.*

Murray, C. K. (2022). A housing supply absorption rate equation. *SSRN Electronic Journal*.

National Geographic Institute. (2025a). *National Plan for Aerial Orthophotography (PNOA): 1m-resolution LiDAR data* [LAZ point cloud].

National Geographic Institute, & National Centre for Geographic Information. (2025b). *Land Information System of Spain (SIPNA) [Geopackages 2018, 2020, 2022, 2023, 2025]*. Ministry of Transport and Sustainable Mobility.

National Statistics Institute. (2025). *Official municipal population figures and demographic variation (Province of Jaén)* [Dataset]. Ministry of Economy, Trade and Business of Spain.

Navarro, B., et al. (2023). Effects of farming system and soil management on floristic diversity in sloping olive groves. *Renewable Agriculture and Food Systems*, 38, e14. https://doi.org/10.1017/S1742170517000096

Occupational Heat Stress Study. (2016). *Universal Thermal Climate Index (UTCI) in outdoor occupational activities*. European Journal of Applied Physiology, 116(9), 1785–1798.

OpenStreetMap contributors. (2025). *OpenStreetMap road networks and urban infrastructure node data for Andalusia* [Data file]. OpenStreetMap Foundation.

Perujo-Villanueva, M., et al. (2017). Land fragmentation and dispersion hampers the optimisation of agricultural management: A case study of traditional olive cultivation in the province of Jaén, Spain. *Biosystems Engineering*, 164, 235–248.

Polyzos, S., & Minetos, D. (2007). Informal Housing in Greece: A Multinomial Logistic Regression Analysis. *Journal of Environmental Planning and Management*, 50(5), 589–612.

Quintas-Soriano, C., Buerkert, A., & Plieninger, T. (2022). Effects of land abandonment on nature contributions to people and good quality of life components in the Mediterranean region: A review. *Land Use Policy*, *116*, 106053. https://doi.org/10.1016/j.landusepol.2022.106053

Ramon y Cajal Abogados. (2021). *Nota sobre la Ley 7/2021, de 1 de diciembre, de impulso para la sostenibilidad del territorio de Andalucía*. Ramon y Cajal Abogados. https://www.ramonycajalabogados.com/es/nota-sobre-la-ley-72021-de-1-de-diciembre-de-impulso-para-la-sostenibilidad-del-territorio-de

Ribeiro, I., Domingos, T., McCracken, D., & Proença, V. (2024). Evaluating Domestic Herbivores for Vegetation Structure Management in Transitional Woodland-Shrubland Systems. *Forests*, 15(12), 2258. https://doi.org/10.3390/f1512225

Regos, A., Pais, S., Campos, J. C., & Lecina-Diaz, J. (2024). Nature-based solutions to wildfires in rural landscapes of Southern Europe: let's be fire-smart! *International Journal of Wildland Fire*, 32(6), 942–956.

Roy, A. (2005). Urban informality: Toward an epistemology of planning. *Journal of the American Planning Association*, 71(2), 147–158. https://doi.org/10.1080/01944360508976689

Rudel, T. K., Coomes, O. T., Moran, E., Achard, F., Angelsen, A., Xu, J., & Lambin, E. (2005). Forest transitions: towards a global understanding of land use change. *Global Environmental Change*, *15*, 23–31. https://doi.org/10.1016/j.gloenvcha.2004.11.001

Ruz Carmona, A. (2025). Estudio de los factores que influyen en los costes del olivar tradicional y estrategias para la mejora de su rentabilidad. Tesis doctoral, Universidad de Jaén

Salis, M., Del Giudice, L., Jahdi, R., Alcasena-Urdiroz, F., Scarpa, C., Pellizzaro, G., Bacciu, V., Schirru, M., Ventura, A., Casula, M., Pedes, F., Canu, A., Duce, P., & Arca, B. (2022). Spatial patterns and intensity of land abandonment drive wildfire hazard and likelihood in Mediterranean agropastoral areas. *Land*, *11*(11), 1942. https://doi.org/10.3390/land11111942

Salvati, L., & Gargiulo Morelli, V. (2014). Unveiling urban sprawl in the Mediterranean region: Towards a latent urban transformation?. *International Journal of Urban and Regional Research*, *38*(6), 1935–1953. https://doi.org/10.1111/1468-2427.12135

Sánchez Martínez, J. D., & Gallego Simón, V. J. (2011). La nueva reconversión productiva del olivar jiennense: Aproximación inicial a sus fundamentos y limitaciones. Cuadernos Geográficos, 49, 95–121

Sanz-Cañada, J. (2014). El aceite de oliva de montaña en Jaén. Calidad y cadena de valor. Instituto de Estudios Giennenses

Serkin, C., & Best, K. (2023). Growth ≠ Density: Zoning Deregulation and the Enduring Problem of Sprawl

Sidle, R., Ziegler, A. The dilemma of mountain roads. *Nature Geosci* **5**, 437–438 (2012). https://doi.org/10.1038/ngeo1512

SoloArquitectura. (2024, 4 de abril). *Requerimientos de la Ley LISTA de Andalucía para construcción de vivienda en terreno rústico*. SoloArquitectura. https://www.soloarquitectura.com/foros/threads/requerimientos-de-ley-lista-de-andalucia-para-construccion-de-vivienda-en-terreno-rustico.125410/

Stock, J. H., & Watson, M. W. (2020). *Introduction to Econometrics* (4th Global ed.). Pearson Education.

van Daalen, K. R., Romanello, M., Rocklöv, J., Semenza, J. C., Tonne, C., Markandya, A., Dasandi, N., Jankin, S., et al. (2022). The 2022 Europe report of the Lancet Countdown on health and climate change: towards a climate resilient future. *The Lancet Public Health*, 7(11), e942–e965. https://doi.org/10.1016/S2468-2667(22)00197-9

Varol, B., Yılmaz, E. Ö., Maktav, D., Bayburt, S., & Gürdal, S. (2019). Detection of illegal constructions in urban cities: comparing LiDAR and stereo KOMPSAT-3 data. *European Journal of Remote Sensing*, 52(1), 387–398. https://doi.org/10.1080/22797254.2019.1604082

Verniz, D., Duarte, J. P., & Queiroz, M. M. (2025). Informal housing settlements and code compliance: the case of Santa Marta favela. *Architecture_MPS*, 31(1), 3. https://doi.org/10.14324/111.444.amps.2025v31i1.003

Walker, R. (2004). Theorizing land-cover and land-use change: The case of tropical deforestation. *International Regional Science Review, 27*(3), 247–270.

Wooldridge, J. M. (2010). *Econometric Analysis of Cross Section and Panel Data* (2nd ed.). MIT Press.

Worklimate 2.0. (2024). *Occupational heat stress adaptation and prevention policies in Italy*. National Research Council (CNR) / Climate-ADAPT. https://climate-adapt.eea.europa.eu/en/metadata/projects/worklimate-2-0-occupational-heat-stress-adaptation-and-prevention-policies

Wiebe, M. (2025). *A two-sector model of land and upzoning*. Michael Wiebe's Blog. https://michaelwiebe.com/blog/2025/07/land_model

7. Appendix

Table A1: Regression Results: Control Variables on Shrubland Cover

	Model 1 (OLS)	**Model 2** (Pure TWFE)	**Model 3** (+ Municipal)	**Model 4** (Final Spec.)
Dependent Variable:	Shrubland Cover (%)			
Constant	42.30*** (0.0774)			
yUTCI_Mun_mean × 2022			0.0948*** (0.0168)	0.0386 (0.0361)
yUTCI_Mun_mean × 2023			0.0300 (0.0184)	-0.0452 (0.0419)
yUTCI_Mun_mean × 2024			-0.0277 (0.0191)	-0.0664 (0.0403)
yUTCI_Mun_mean × 2025			0.0048 (0.0187)	-0.0229 (0.0350)
TasaCrecimiento × 2022			-0.0314*** (0.0075)	-0.0285* (0.0151)
TasaCrecimiento × 2023			-0.0177 (0.0108)	-0.0190 (0.0165)
TasaCrecimiento × 2024			-0.0244** (0.0110)	-0.0315** (0.0142)
TasaCrecimiento × 2025			-0.0242** (0.0111)	-0.0257 (0.0164)
area_ha × 2022				0.3710*** (0.1179)
area_ha × 2023				0.0243 (0.0992)
area_ha × 2024				-0.0830 (0.1007)
area_ha × 2025				-0.0669 (0.0999)
alt_mean × 2022				-0.0008 (0.0017)
alt_mean × 2023				-0.0042** (0.0016)
alt_mean × 2024				-0.0030* (0.0018)
alt_mean × 2025				-0.0015 (0.0018)
slp_mean × 2022				-0.0267 (0.0220)
slp_mean × 2023				0.0060 (0.0192)
slp_mean × 2024				0.0059 (0.0228)
slp_mean × 2025				-0.0144 (0.0173)
Irrigated × 2022				-0.3724 (0.6660)
Irrigated × 2023				-0.0328 (0.6271)
Irrigated × 2024				-0.2930 (0.6495)
Irrigated × 2025				-0.1545 (0.6462)

Continued on next page

Table A1: Regression Results: Control Variables on Shrubland Cover (continued)

	Model 1 (OLS)	**Model 2** (Pure TWFE)	**Model 3** (+ Municipal)	**Model 4** (Final Spec.)
Dependent Variable:		Shrubland Cover (%)		
disturb_mean × 2022				0.0007^{***}
				(0.0001)
disturb_mean × 2023				0.0006^{***}
				(0.0002)
disturb_mean × 2024				3.59×10^{-5}
				(0.0002)
disturb_mean × 2025				0.0001
				(0.0002)
distcarr_mean × 2022				-0.0005
				(0.0017)
distcarr_mean × 2023				0.0008
				(0.0020)
distcarr_mean × 2024				0.0033^{*}
				(0.0020)
distcarr_mean × 2025				0.0040^{*}
				(0.0020)
HubDist × 2022				-5.39×10^{-5}
				(7.60×10^{-5})
HubDist × 2023				-5.73×10^{-5}
				(7.10×10^{-5})
HubDist × 2024				-0.0001
				(8.47×10^{-5})
HubDist × 2025				-3.98×10^{-5}
				(7.55×10^{-5})
Fixed Effects				
Plot FE (`id_0`)	No	Yes	Yes	Yes
Year FE (`ano`)	No	Yes	Yes	Yes
Fit Statistics				
Standard Errors (S.E.)	IID	Clustered (`id_0`)	Clustered (`id_0`)	Clustered (`id_ine`)
Observations	157,895	157,895	157,895	157,895
R^2	0.02020	0.57549	0.57586	0.57766
Within R^2	—	0.00097	0.00185	0.00609

Notes: The dependent variable is `matorral_pct` (expressed as a percentage). Standard errors are reported in parentheses below the estimated coefficients. Significance codes: *** $p < 0.01$, ** $p < 0.05$, * $p < 0.1$.

Table A2: Full Robustness Checks: All Models and Control Variables

	Model 1 (Baseline M4)	**Model 2** (Latif. Trim)	**Model 3** (Plot Cluster)	**Model 4** (Spatial Jack.)	**Model 5** (Min. Dist.)	**Model 6** (Non-Linear)
Dependent Variable:	Shrubland Cover (%)					
LISTA_Treat × 2022	-0.6451	-0.2894	-0.6451*	-0.6409	-0.6474	-0.3697
	(0.6580)	(0.6487)	(0.3463)	(0.6853)	(0.6584)	(0.6422)
LISTA_Treat × 2023	0.0590	0.0185	0.0590	0.0557	0.0648	0.0630
	(0.6666)	(0.6702)	(0.3881)	(0.7017)	(0.6666)	(0.6692)
LISTA_Treat × 2024	1.216*	1.163*	1.216***	1.124	1.226*	1.258*
	(0.6544)	(0.6647)	(0.3934)	(0.6781)	(0.6546)	(0.6631)
LISTA_Treat × 2025	1.202*	1.118*	1.202***	1.301*	1.218*	1.219*
	(0.6522)	(0.6471)	(0.3865)	(0.6734)	(0.6512)	(0.6318)
yUTCI_Mun_mean × 2022	0.0386	0.0305	0.0386**	0.0416	0.0390	0.0094
	(0.0361)	(0.0359)	(0.0186)	(0.0372)	(0.0361)	(0.0348)
yUTCI_Mun_mean × 2023	-0.0452	-0.0441	-0.0452**	-0.0481	-0.0440	-0.0711*
	(0.0419)	(0.0435)	(0.0201)	(0.0428)	(0.0418)	(0.0411)
yUTCI_Mun_mean × 2024	-0.0664	-0.0668	-0.0664***	-0.0716*	-0.0654	-0.0993**
	(0.0403)	(0.0404)	(0.0208)	(0.0414)	(0.0403)	(0.0399)
yUTCI_Mun_mean × 2025	-0.0229	-0.0179	-0.0229	-0.0314	-0.0218	-0.0538
	(0.0350)	(0.0356)	(0.0204)	(0.0348)	(0.0352)	(0.0347)
TasaCrecimiento × 2022	-0.0285*	-0.0293**	-0.0285***	-0.0261	-0.0284*	-0.0239
	(0.0151)	(0.0147)	(0.0076)	(0.0161)	(0.0151)	(0.0154)
TasaCrecimiento × 2023	-0.0190	-0.0209	-0.0190*	-0.0182	-0.0191	-0.0148
	(0.0165)	(0.0160)	(0.0110)	(0.0170)	(0.0165)	(0.0169)
TasaCrecimiento × 2024	-0.0315**	-0.0310**	-0.0315***	-0.0330**	-0.0316**	-0.0263*
	(0.0142)	(0.0145)	(0.0112)	(0.0140)	(0.0143)	(0.0155)
TasaCrecimiento × 2025	-0.0257	-0.0281*	-0.0257**	-0.0273*	-0.0257	-0.0210
	(0.0164)	(0.0158)	(0.0113)	(0.0162)	(0.0164)	(0.0174)
area_ha × 2022	0.3710***	1.444***	0.3710***	0.3572***	0.3725***	0.7143***
	(0.1179)	(0.2047)	(0.1060)	(0.1130)	(0.1185)	(0.1229)
area_ha × 2023	0.0243	-0.0414	0.0243	0.0227	0.0264	-0.1657
	(0.0992)	(0.2081)	(0.0810)	(0.1002)	(0.0983)	(0.1319)
area_ha × 2024	-0.0830	-0.2508	-0.0830	-0.0849	-0.0790	-0.2470
	(0.1007)	(0.2681)	(0.0738)	(0.1017)	(0.0993)	(0.1545)
area_ha × 2025	-0.0669	-0.2767	-0.0669	-0.0655	-0.0619	-0.2656*
	(0.0999)	(0.2447)	(0.0775)	(0.1002)	(0.0984)	(0.1494)
alt_mean × 2022	-0.0008	-0.0003	-0.0008	-0.0008	-0.0009	-0.0163**
	(0.0017)	(0.0017)	(0.0009)	(0.0018)	(0.0017)	(0.0072)
alt_mean × 2023	-0.0042**	-0.0041**	-0.0042***	-0.0046***	-0.0042***	-0.0207**
	(0.0016)	(0.0016)	(0.0010)	(0.0016)	(0.0016)	(0.0087)
alt_mean × 2024	-0.0030*	-0.0033*	-0.0030***	-0.0035*	-0.0031*	-0.0235***
	(0.0018)	(0.0018)	(0.0010)	(0.0018)	(0.0018)	(0.0084)
alt_mean × 2025	-0.0015	-0.0014	-0.0015	-0.0021	-0.0015	-0.0207**
	(0.0018)	(0.0018)	(0.0010)	(0.0017)	(0.0018)	(0.0081)
slp_mean × 2022	-0.0267	-0.0240	-0.0267**	-0.0299	-0.0268	-0.1427**
	(0.0220)	(0.0228)	(0.0134)	(0.0228)	(0.0220)	(0.0584)
slp_mean × 2023	0.0060	0.0041	0.0060	0.0059	0.0066	-0.0432
	(0.0192)	(0.0199)	(0.0147)	(0.0201)	(0.0192)	(0.0605)
slp_mean × 2024	0.0059	0.0048	0.0059	0.0042	0.0056	-0.0587
	(0.0228)	(0.0225)	(0.0155)	(0.0237)	(0.0228)	(0.0567)
slp_mean × 2025	-0.0144	-0.0146	-0.0144	-0.0138	-0.0147	-0.0338
	(0.0173)	(0.0176)	(0.0153)	(0.0179)	(0.0174)	(0.0593)
Irrigated × 2022	-0.3724	-0.2971	-0.3724	-0.4720	-0.3693	-0.4132
	(0.6660)	(0.6647)	(0.4367)	(0.6700)	(0.6677)	(0.6565)
Irrigated × 2023	-0.0328	0.0436	-0.0328	0.0693	-0.0329	-0.1290
	(0.6271)	(0.6156)	(0.5118)	(0.6214)	(0.6254)	(0.6411)
Irrigated × 2024	-0.2930	-0.3379	-0.2930	-0.1362	-0.2778	-0.4226
	(0.6495)	(0.6532)	(0.5306)	(0.6374)	(0.6459)	(0.6545)
Irrigated × 2025	-0.1545	-0.1039	-0.1545	-0.1112	-0.1352	-0.2804
	(0.6462)	(0.6485)	(0.5040)	(0.6547)	(0.6456)	(0.6487)
disturb_mean × 2022	0.0007***	0.0007***	0.0007***	0.0007***		0.0007***
	(0.0001)	(0.0001)	(9.41×10^{-5})	(0.0001)		(0.0001)

Continued on next page

Table A2: Full Robustness Checks: All Models (continued)

	Model 1 (Baseline M4)	Model 2 (Latif. Trim)	Model 3 (Plot Cluster)	Model 4 (Spatial Jack.)	Model 5 (Min. Dist.)	Model 6 (Non-Linear)
Dependent Variable:	Shrubland Cover (%)					
disturb_mean × 2023	0.0006^{***}	0.0006^{***}	0.0006^{***}	0.0005^{***}		0.0006^{***}
	(0.0002)	(0.0002)	(0.0001)	(0.0002)		(0.0002)
disturb_mean × 2024	3.59×10^{-5}	7.80×10^{-5}	3.59×10^{-5}	5.57×10^{-6}		6.14×10^{-5}
	(0.0002)	(0.0001)	(9.70×10^{-5})	(0.0001)		(0.0001)
disturb_mean × 2025	0.0001	0.0001	0.0001	0.0001		0.0002
	(0.0002)	(0.0003)	(0.0001)	(0.0002)		(0.0002)
distcarr_mean × 2022	-0.0005	-0.0015	-0.0005	-0.0009		-0.0008
	(0.0017)	(0.0018)	(0.0014)	(0.0018)		(0.0018)
distcarr_mean × 2023	0.0008	0.0008	0.0008	0.0005		0.0008
	(0.0020)	(0.0021)	(0.0015)	(0.0021)		(0.0021)
distcarr_mean × 2024	0.0033^{*}	0.0031	0.0033^{**}	0.0028		0.0032
	(0.0020)	(0.0020)	(0.0015)	(0.0020)		(0.0020)
distcarr_mean × 2025	0.0040^{*}	0.0042^{**}	0.0040^{**}	0.0033		0.0040^{*}
	(0.0020)	(0.0021)	(0.0016)	(0.0020)		(0.0021)
HubDist × 2022	-5.39×10^{-5}	-6.60×10^{-5}	-5.39×10^{-5}	-6.23×10^{-5}	-5.39×10^{-5}	-5.19×10^{-5}
	(7.60×10^{-5})	(7.55×10^{-5})	(3.37×10^{-5})	(7.58×10^{-5})	(7.60×10^{-5})	(7.34×10^{-5})
HubDist × 2023	-5.73×10^{-5}	-5.87×10^{-5}	-5.73×10^{-5}	-4.79×10^{-5}	-5.66×10^{-5}	-4.61×10^{-5}
	(7.10×10^{-5})	(7.04×10^{-5})	(3.79×10^{-5})	(7.12×10^{-5})	(7.08×10^{-5})	(6.80×10^{-5})
HubDist × 2024	-0.0001	-9.67×10^{-5}	-0.0001^{***}	-9.96×10^{-5}	-0.0001	-9.15×10^{-5}
	(8.47×10^{-5})	(8.43×10^{-5})	(3.87×10^{-5})	(8.59×10^{-5})	(8.48×10^{-5})	(8.18×10^{-5})
HubDist × 2025	-3.98×10^{-5}	-4.46×10^{-5}	-3.98×10^{-5}	-2.96×10^{-5}	-3.97×10^{-5}	-2.53×10^{-5}
	(7.55×10^{-5})	(7.73×10^{-5})	(3.82×10^{-5})	(7.62×10^{-5})	(7.56×10^{-5})	(7.07×10^{-5})
disturb_min × 2022					0.0007^{***}	
					(0.0001)	
disturb_min × 2023					0.0005^{***}	
					(0.0002)	
disturb_min × 2024					2.95×10^{-5}	
					(0.0001)	
disturb_min × 2025					0.0001	
					(0.0002)	
distcarr_min × 2022					-0.0005	
					(0.0019)	
distcarr_min × 2023					-0.0007	
					(0.0022)	
distcarr_min × 2024					0.0027	
					(0.0020)	
distcarr_min × 2025					0.0034	
					(0.0022)	
I(area_ha^2) × 2022						-0.0041^{***}
						(0.0008)
I(area_ha^2) × 2023						0.0022^{**}
						(0.0008)
I(area_ha^2) × 2024						0.0018^{*}
						(0.0011)
I(area_ha^2) × 2025						0.0023^{**}
						(0.0011)
I(alt_mean^2) × 2022						$1.06 \times 10^{-5**}$
						(4.39×10^{-6})
I(alt_mean^2) × 2023						$1.10 \times 10^{-5*}$
						(5.54×10^{-6})
I(alt_mean^2) × 2024						$1.36 \times 10^{-5**}$
						(5.33×10^{-6})
I(alt_mean^2) × 2025						$1.27 \times 10^{-5**}$
						(4.90×10^{-6})
I(slp_mean^2) × 2022						0.0032^{***}
						(0.0012)
I(slp_mean^2) × 2023						0.0014
						(0.0014)

Continued on next page

Table A2: Full Robustness Checks: All Models (continued)

	Model 1 (Baseline M4)	Model 2 (Latif. Trim)	Model 3 (Plot Cluster)	Model 4 (Spatial Jack.)	Model 5 (Min. Dist.)	Model 6 (Non-Linear)
Dependent Variable:			Shrubland Cover (%)			
I(slp_mean^2) × 2024						0.0018 (0.0013)
I(slp_mean^2) × 2025						0.0006 (0.0015)
Fixed Effects						
Plot FE (id_0)	Yes	Yes	Yes	Yes	Yes	Yes
Year FE (ano)	Yes	Yes	Yes	Yes	Yes	Yes
Fit Statistics						
S.E. Clustered by:	id_ine	id_ine	id_0	id_ine	id_ine	id_ine
Observations	157,895	156,315	157,895	150,380	157,895	157,895
R^2	0.57766	0.57998	0.57766	0.57591	0.57764	0.57861
Within R^2	0.00609	0.00748	0.00609	0.00635	0.00605	0.00832

Notes: Standard errors clustered at the level specified at the bottom are reported in parentheses. Significance codes: *** $p < 0.01$, ** $p < 0.05$, * $p < 0.1$.